Am J Nucl Med Mol Imaging 2021;11(6):443-475
www.ajnmmi.us /ISSN:2160-8407/ajnmmi0138820

*Review Article*

# A review of advances in the last decade on targeted cancer therapy using $^{177}$Lu: focusing on $^{177}$Lu produced by the direct neutron activation route

Rubel Chakravarty[1,2], Sudipta Chakraborty[1,2]

[1]*Radiopharmaceuticals Division, Bhabha Atomic Research Centre, Trombay, Mumbai 400085, India;* [2]*Homi Bhabha National Institute, Anushaktinagar, Mumbai 400094, India*

Received September 2, 2021; Accepted October 9, 2021; Epub December 15, 2021; Published December 30, 2021

**Abstract:** Lutetium-177 [$T_{½}$ = 6.76 d; $E_{β}$ (max) = 0.497 MeV; maximum tissue range ~2.5 mm; 208 keV γ-ray] is one of the most important theranostic radioisotope used for the management of various oncological and non-oncological disorders. The present review chronicles the advancement in the last decade in $^{177}$Lu-radiopharmacy with a focus on $^{177}$Lu produced via direct $^{176}$Lu (n, γ) $^{177}$Lu nuclear reaction in medium flux research reactors. The specific nuances of $^{177}$Lu production by various routes are described and their pros and cons are discussed. Lutetium, is the last element in the lanthanide series. Its chemistry plays a vital role in the preparation of a wide variety of radiopharmaceuticals which demonstrate appreciable *in vivo* stability. Traditional bifunctional chelators (BFCs) that are used for $^{177}$Lu-labeling are discussed and the upcoming ones are highlighted. Research efforts that resulted in the growth of various $^{177}$Lu-based radiopharmaceuticals in preclinical and clinical settings are provided. This review also summarizes the results of clinical studies with potent $^{177}$Lu-based radiopharmaceuticals that have been prepared using medium specific activity $^{177}$Lu produced by direct neutron activation route in research reactors. Overall, the review amply demonstrates the practicality of the medium specific activity $^{177}$Lu towards formulation of various clinically useful radiopharmaceuticals, especially for the benefit of millions of cancer patients in developing countries with limited reactor facilities.

**Keywords:** $^{177}$Lu, direct neutron activation, DOTATATE, intrinsically radiolabeled nanoparticles, medium flux research reactors, specific activity, PSMA-617, targeted therapy, TENIS

## Introduction

Over the last several decades, the production and application of radiometals have matured from largely ambiguous and experimental technologies to indispensable components of routine practices in nuclear medicine. This transition has been driven by the mutually essential advances in radiochemical processing, biomedical sciences, synthetic organic and inorganic chemistry, nuclear imaging technology and cancer biology. Radiometals which are γ-emitters or positron emitters are generally used for diagnostic applications utilizing single photon emission computed tomography (SPECT) or positron emission tomography (PET) imaging modalities. Contrastingly, particulate emitting radiometals (α, $β^-$, conversion and/or Auger electrons) are in high demand for internal radiotherapy. Dosimetry is the major challenge with internal radiotherapy due to uncertainty in measurement of radiation dose associated with particulate radiation from outside the patient body. To circumvent this limitation, presently efforts are emerging towards combining the diagnosis (molecular imaging) and the internal radiotherapy (molecular targeted therapy) and this concept is known as "theranostics" [1-5].

The fundamental requirement of theranostics is that the same or similar chemical compound should be labelled with a diagnostic and a therapeutic radionuclide. For the diagnostic part of the investigation, SPECT and PET imaging techniques are used. To meet the requirement of theranostics, the two radionuclides chosen are preferably of the same chemical element, even

**Table 1.** Nuclear decay characteristics of some intrinsically theranostic radiometals

| Radiometal | Decay mode | $T_{½}$ (h) | $E_{max}$ (β), MeV (%) | Principal γ-energy, keV (%) | Mean tissue range (mm) |
|---|---|---|---|---|---|
| $^{47}$Sc | $β^-$, γ | 80.4 | 0.60 (100) | 159.4 (68) | 0.20 |
| $^{64}$Cu | $β^+$, $β^-$, γ (EC) | 12.7 | $β^+$: 0.65 (19)<br>$β^-$: 0.58 (40) | 511 (38.6) | 0.19 |
| $^{67}$Cu | $β^-$, γ | 61.9 | 0.58 (100) | 184.6 (46.7)<br>93.3 (16.6)<br>91.3 (7.3) | 0.19 |
| $^{153}$Sm | $β^-$, γ | 46.3 | 0.81 (100) | 103 (28.3) | 0.30 |
| $^{161}$Tb | $β^-$, γ | 165.8 | 0.59 (100) | 48.9 (17.0)<br>74.6 (10.2) | 0.20 |
| $^{166}$Ho | $β^-$, γ | 26.8 | 1.86 (100) | 80.6 (6.2) | 0.84 |
| $^{177}$Lu | $β^-$, γ | 161.0 | 0.50 (100) | 208 (11)<br>113 (6.6) | 0.16 |
| $^{186}$Re | $β^-$, γ | 89.2 | 1.10 (92.5) | 137 (9) | 0.43 |
| $^{188}$Re | $β^-$, γ | 16.9 | 2.10 (100) | 155 (15) | 0.98 |

though chemically similar elements are also utilized occasionally. A more preferable option in this regard is to use intrinsically theranostic radiometals which by virtue of their suitable γ or $β^+$ emission can be used for diagnostic imaging and due to suitable particulate emission can be used for targeted therapy. The use of the same radiometal would give an accurate idea regarding the pharmacokinetics of the radiopharmaceutical administered for dosimetric estimation.

Several intrinsically theranostic radiometals such as $^{47}$Sc, $^{64}$Cu, $^{67}$Cu, $^{153}$Sm, $^{166}$Ho, $^{177}$Lu, $^{186}$Re, etc., with fascinating nuclear decay characteristics (as summarized in **Table 1**) have been studied for preparation of radiopharmaceuticals in preclinical and clinical settings [6-10]. Although nuclear decay characteristics are of paramount importance for selection of an intrinsically theranostic radiometal, its success in real clinical context also depends on the practicality of large-scale production with acceptable purity and the supply logistics. In this regard, $^{177}$Lu has numerous advantages in comparison to other intrinsically theranostic radiometals [11, 12]. The nuclear decay properties of $^{177}$Lu such as its relatively long half-life, the energy of $β^-$ particles and the energy and abundance of the γ-photons make it suitable for use in preparation of theranostic radiopharmaceuticals for targeting small-sized primary tumors and their metastatic sites [12].

Clinical efficacies of several $^{177}$Lu-based radiopharmaceuticals have been established in different parts of the world [12]. A quick "Pubmed" search shows that more than 1500 papers have been published in the last decade on $^{177}$Lu-based radiopharmaceuticals and their utilization in preclinical and clinical settings. In this review, our objective to provide an apt and wide-ranging overview of the $^{177}$Lu-based radiopharmaceuticals developed over the last one decade, with focus on utilization of $^{177}$Lu produced via direct neutron activation route. The choice of BFCs which are used for $^{177}$Lu-labeling to the different carrier molecules are discussed. The development of various ligands and nanoconstructs for site- and event-specific targeting are summarized, and the likelihood and fascinating opportunities for future development which might help in translating this exciting research area towards routine clinical use are discussed.

## Production of $^{177}$Lu

Lutetium-177 is among the very few radioisotopes that can be produced both in a cyclotron as well as in a nuclear reactor. The schematic illustrating the production of $^{177}$Lu in a cyclotron and nuclear reactor is shown in **Figure 1**. The cyclotron production route is relatively less explored because of the low batch yields of the process which is unsuitable to meet the clinical demands. Nevertheless, it is feasible approach to produce $^{177}$Lu of equivalent quality without depending on nuclear reactors to fulfil the requirements of research and development laboratories and academic institutions. The details of production of $^{177}$Lu by various produc-

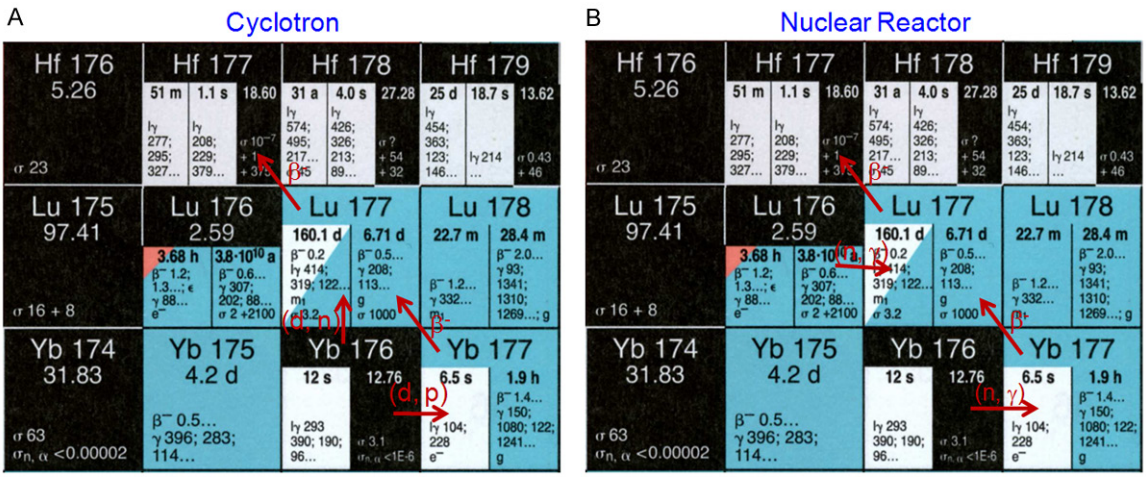


**Figure 1.** Production of $^{177}$Lu in (A) cyclotron via $^{176}$Yb (d, n) $^{177}$Lu and $^{176}$Yb (d, p) $^{177}$Yb→$^{177}$Lu reactions and (B) nuclear reactor via $^{176}$Lu (n, γ) $^{177}$Lu and $^{176}$Yb (n, γ) $^{177}$Yb→$^{177}$Lu reactions.

tion methodologies in nuclear reactor or cyclotron are dealt with in the following sections.

*Cyclotron production route*

The production of $^{177}$Lu in a cyclotron has been explored more from an academic perspective. For the first time, Hermanne et al. studied the deuteron induced nuclear reactions for production of no-carrier-added (NCA) Lu radioisotopes and reported the excitation functions for their formation [13]. Similar results were also reported by Maneti et al. and Khandaker et al. [14, 15]. In these studies, stacked foil activation technique on natural Yb targets at incident deuteron energies up to 20 MeV was explored. The authors inferred from these studies that two different nuclear reactions, viz., $^{176}$Yb (d, n) $^{177}$Lu and $^{176}$Yb (d, p) $^{177}$Yb→$^{177}$Lu, contributed to the generation of $^{177}$Lu by deutron bombardment on Yb target. By analysis of the excitation functions, it was revealed that the principal route for the production of $^{177}$Lu was the indirect nuclear reaction $^{176}$Yb (d, p) $^{177}$Yb→$^{177}$Lu, where co-production of $^{177m}$Lu impurity ($T_{½}$ = 160.5 d) could be minimized [16, 17]. Kambali calculated that the end of bombardment (EOB) yields for the direct i.e. $^{176}$Yb (d, n) $^{177}$Lu reaction and indirect i.e. $^{176}$Yb (d, p) $^{177}$Yb reaction were 0.519 and 181.1 MBq/μA h, respectively [17]. In order to enhance the overall yield of $^{177}$Lu and minimize the radionuclidic impurities due to extraneous Lu radioisotopes, highly enriched $^{176}$Yb target must be used. Use of enriched $^{176}$Yb could yield $^{177}$Lu free from other coproduced $^{177}$Lu radionuclides such as $^{170}$Lu, $^{171}$Lu, $^{172}$Lu, $^{173}$Lu and $^{174}$Lu [12].

In another approach, Medvedev et al. investigated the feasibility of production of $^{177}$Lu in a proton accelerator by irradiation of Ta and Hf targets [18]. The authors reported both theoretical and experimental activation cross-sections of proton induced reactions at 100 and 200 MeV proton beam energy. The largest cross-section of ~20 mb was found for the Hf target at 195 MeV proton energy. In addition to the small reaction cross-section, a major shortcoming of this approach is the co-production of extraneous Lu isotopes reducing the specific activity and radionuclidic purity required for the practical applications.

*Reactor production route*

Two independent routes are adopted for production of $^{177}$Lu in nuclear reactors and these are the most commonly used methods for large-scale production of $^{177}$Lu for therapeutic purposes world over [11, 19]. The first is the "direct" production of $^{177}$Lu via $^{176}$Lu (n, γ) $^{177}$Lu reaction in medium to high flux research reactors. The other approach involves "indirect" production of $^{177}$Lu via $^{176}$Yb (n, γ) $^{177}$Yb→$^{177}$Lu by irradiating enriched $^{176}$Yb target in high flux research reactors. In the direct route, the post irradiation radiochemical processing involves simple dissolution of the irradiated target, whereas, the indirect route involves radiochemical separation of $^{177}$Lu from the bulk irra-

diated Yb target. The major advantage of the indirect route is that it yields NCA $^{177}$Lu and the product is free from the long-lived radionuclidic impurity, $^{177m}$Lu. However, the success of this method depends on availability of a suitable method for radiochemical separation of miniscule quantities (in μg level) of NCA $^{177}$Lu from bulk irradiated Yb target (in g quantities). Since, Lu and Yb are adjacent members of the lanthanide series, their chemical properties are similar which makes the separation process quite challenging. Over the last several years numerous methods of radiochemical separation based on solvent extraction, ion exchange, electrochemical technique, either alone or in combination have been reported for separation of NCA $^{177}$Lu from the irradiated target [20-28]. All these methods involve laboratory scale separation and the details of large-scale separation in industrial settings to meet the surging demand of the nuclear medicine departments have not yet been reported. As a result, the technology for production of NCA $^{177}$Lu is not available to most of the countries and the radioisotope is supplied by few commercial manufacturers, which restricts it widespread clinical utility.

Generally, highly enriched (>98%) $^{176}$Yb target is required for the production of NCA $^{177}$Lu by the indirect route. This is because the natural abundance of $^{176}$Yb is only 12.6%. Irradiation of natural Yb target will not only result in lower production yield but also lead to production of significantly higher activity level of $^{175}$Yb, which will increase the radiation dose to working personnel during target processing and radiochemical separation. Moreover, on irradiation of natural Yb target, some stable isotopes of Lu will be produced as decay products which will significantly lower the specific activity of $^{177}$Lu obtained after radiochemical separation. Use of highly enriched target would lead to the production of NCA $^{177}$Lu with specific activity approaching the theoretical value of ~110 Ci (4.1 TBq)/g [12, 20]. Considering the contribution due to thermal neutron capture only, the activity of NCA $^{177}$Lu produced by indirect route can be calculated using the following equations:

$$N(t) = No\Lambda_1^* \Lambda_2^* \left[\frac{\exp(-\Lambda_1 t)}{(\Lambda_2 - \Lambda_1)(\Lambda_3 - \Lambda_1)} + \frac{\exp(-\Lambda_2 t)}{(\Lambda_1 - \Lambda_2)(\Lambda_3 - \Lambda_2)} + \frac{\exp(-\Lambda_3 t)}{(\Lambda_1 - \Lambda_3)(\Lambda_2 - \Lambda_3)}\right] \quad (1)$$

$$A(t) = N(t) \times \lambda_3(t) \quad (2)$$

$$\Lambda_1^* = \Lambda_1 = \sigma_1 \Phi \quad (3)$$

$$\Lambda_2^* = \Lambda_2 = \lambda_2 \quad (4)$$

$$\Lambda_3 = \sigma_3 \Phi + \lambda_3 \quad (5)$$

where, $N_o$ is the number of $^{176}$Yb atoms used as target (at t = 0), A (t) is the activity of $^{177}$Lu produced after irradiation for time 't', $\sigma_1$ is the thermal neutron capture cross-section of $^{175}$Yb, $\sigma_3$ is the thermal neutron capture cross-section of $^{177}$Lu, $\lambda_2$ is the decay constant of $^{177}$Yb, $\lambda_3$ is the decay constant of $^{177}$Lu, Φ is the flux of the reactor.

Contrarily, while calculating the $^{177}$Lu activity produced via direct $^{176}$Lu (n, γ) $^{177}$Lu reaction, two noteworthy effects have to be considered [11]. First, significant target burn up is caused due to the high cross section of $^{176}$Lu and therefore the number of target atoms does not remain constant during the course of irradiation. Second, the reaction cross section, which is a function of neutron velocity [σ ($v_n$)], exhibits a strong resonance at 0.1413 eV and therefore it deviates from the $1/v_n$ law. For such situations, the Westcott convention has to be adopted for calculating the activity produced [29]:

$$A = \frac{No\sigma_1 \phi k \lambda}{\lambda + \phi(\sigma_2 - \sigma_1 k)}\left[\exp\left\{-\sigma_1 k \phi t\right\} - \exp\left\{-(\lambda + \sigma_2 \phi)t\right\}\right] \quad (6)$$

where, $N_o$ is the number of $^{176}$Lu atoms used as target (at t = 0), λ the decay constant of $^{177}$Lu (in $s^{-1}$), $\sigma_1$ the thermal neutron capture cross section of $^{176}$Lu at the neutron velocity of 2,200 $ms^{-1}$ (2,090 b), $\sigma_2$ is the thermal neutron capture cross section of $^{177}$Lu at the neutron velocity of 2,200 $ms^{-1}$ (1,000 b), Φ the thermal neutron flux of the reactor (in $cm^{-2}s^{-1}$), t is the time of irradiation and 'k' is so called k-factor which can be expressed as:

$$k = [G_{th}.g(T_n) + G_r.r(\alpha)\sqrt{T_n/T_0}.s_o(\alpha)] \quad (7)$$

Where, $G_{th}$ is the thermal neutron self-shielding factor, $G_r$ is the epithermal neutron self-shielding factor, g ($T_n$) is the Westcott factor with thermal neutron temperature $T_n$, r (α) $\sqrt{T_n/T_0}$ . is the Westcott spectral index, $s_o$ (α) is the $s_o$ $(E_r)^{-\alpha}$, where $s_o$ and $E_r$ are constants. The k-factor depends upon several parameters such as, thermal energy cross-section at a reference temperature, resonance integral, epithermal

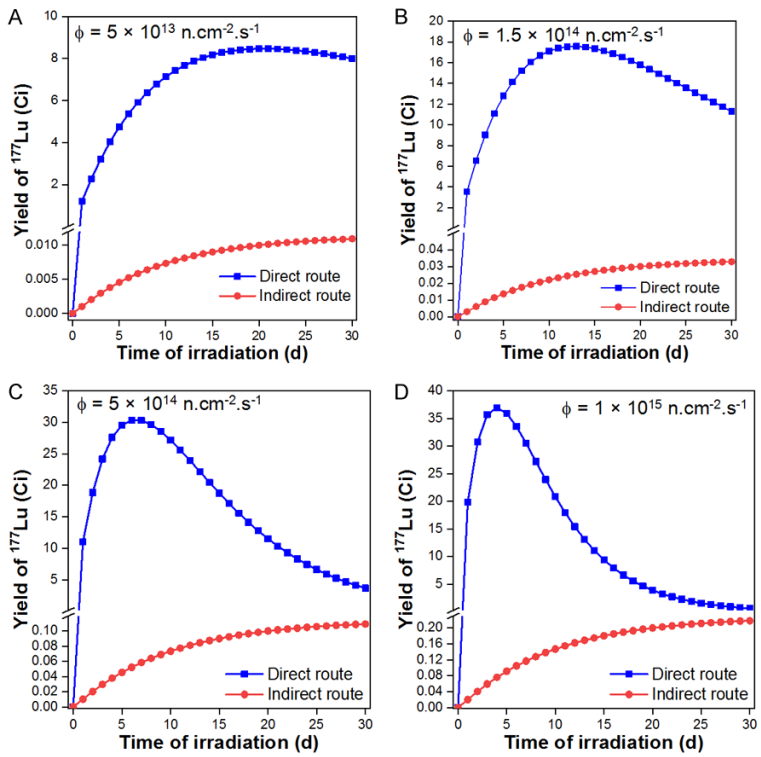


**Figure 2.** Comparative evaluation of the yield of $^{177}$Lu produced via direct $^{176}$Lu (n, γ) $^{177}$Lu and indirect $^{176}$Yb (n, γ) $^{177}$Yb→$^{177}$Lu routes when irradiated at flux of (A) 5 × $10^{13}$ n.cm$^{-2}$.s$^{-1}$, (B) 1.5 × $10^{14}$ n.cm$^{-2}$.s$^{-1}$, (C) 5 × $10^{14}$ n.cm$^{-2}$.s$^{-1}$ and (D) 1 × $10^{15}$ n.cm$^{-2}$.s$^{-1}$ for different irradiation times.

index, epithermal flux shape factor, Westcott g-factor, temperature, Cadmium cut-off energy, effective resonance energy and flux attenuation factor for thermal and epithermal neutrons [29]. Generally, the value of 'k' is reported to be between 1.5 and 2.5 [30].

Since, the natural abundance of $^{176}$Lu is only 2.6%, enriched lutetium target (>70% enriched in $^{176}$Lu) is required for production of $^{177}$Lu with adequate specific activity by the direct route. Owing to the large cross-section, the consumption of the target in a typical batch is very low. Generally, 25-100 μg of $^{176}$Lu target is required for production of 37 GBq (1 Ci) of $^{177}$Lu depending on the flux of the reactor. The yields of $^{177}$Lu produced by the direct and indirect route on irradiation of 1 mg each of $Lu_2O_3$ (80% enriched in $^{176}$Lu) and $Yb_2O_3$ (99.9% enriched in $^{176}$Yb) targets, respectively, under different flux conditions were calculated using equations 1 and 6 and plotted in **Figure 2**. For simplicity, only the thermal neutron contribution was considered in both the cases and the k-factor was assumed as 1.75. It can be seen from the figures that production of $^{177}$Lu by the direct route requires cautious optimization of the time of irradiation, which diverges between 5-20 days depending on the flux of the reactor. Under the optimal conditions, the specific activity of >740 GBq (20 Ci)/mg can easily be achieved in the direct production route on irradiation in medium flux research reactor (Φ >$10^{14}$ n.cm$^{-2}$.s$^{-1}$). In sharp contrast to the direct production route, the yield of $^{177}$Lu in the indirect route is drastically lower based on the target mass at all flux conditions. This significantly increases the cost of production of $^{177}$Lu by the indirect route, as the process involves the use of highly enriched target and the reaction cross-section is low (2.85 b). Additionally, the process involves intricate radiochemical separation which further escalates the cost. Utilization of enriched targets for radioisotope production involving low activation cross-section reaction is not a viable proposition, as considerable portion of the target does not capture neutrons. As seen from **Figure 2**, it is advisable to produce $^{177}$Lu by the indirect route only if there is access to high flux research reactor (Φ >5 × $10^{14}$ n.cm$^{-2}$.s$^{-1}$) for radioisotope production. Even then, the process would be practical only if there is provision to efficiently recover the unused enriched target after the radiochemical separation. According the International Atomic Energy Agency database, majority of the operational research reactors for isotope production are medium flux research reactors [31]. For its widespread utilization, $^{177}$Lu can be cost-effectively produced by the direct route in these medium flux research reactors. Nevertheless, NCA $^{177}$Lu produced in large-scale in high flux research reactors is available commercially and is preferred by certain groups.

A major concern with $^{177}$Lu produced by the direct route is the co-production of small amount of long-lived $^{177m}$Lu as the radionuclidic impurity [11]. Owing to the low cross-section (~7 b) of the $^{176}$Lu (n, γ) $^{177m}$Lu reaction and the

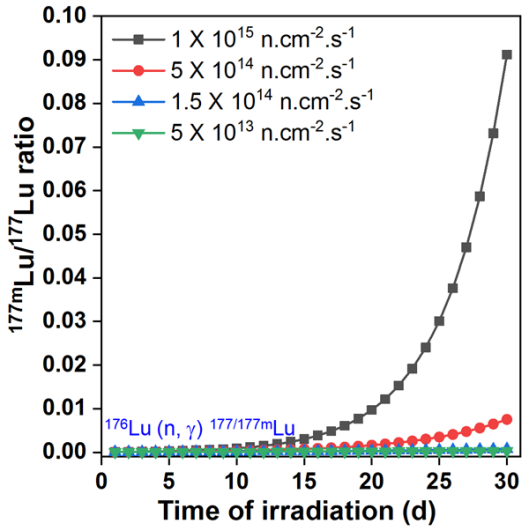


**Figure 3.** Calculated $^{177m}$Lu/$^{177}$Lu ratios during production of $^{177}$Lu via direct $^{176}$Lu (n, γ) $^{177}$Lu route when irradiated at different fluxes for different irradiation times in nuclear reactor.

long half-life of the radioisotope, the yield of $^{177m}$Lu is relatively low under most irradiation conditions. **Figure 3** shows the activity of $^{177m}$Lu co-produced at different thermal neutron flux values when irradiated for different time periods. Especially, under medium flux conditions the level of $^{177m}$Lu in $^{177}$Lu is <0.02% and is therefore not a significant issue [12]. Lutetium-177m, being a radionuclidic impurity, is taken up in the same tissues where the uptake of $^{177}$Lu-based radiopharmaceutical occurs. However, its duration of retention in the tissues will be much more prolonged compared to $^{177}$Lu because of its much longer half-life. Moreover, if metabolization of the targeting agent occurs, free $^{177m}$Lu can be excreted or skeletal uptake may occur. This is not a cause of much concern as the radiation dose due to $^{177m}$Lu will be low. However, from waste management point of view, the presence of $^{177m}$Lu in $^{177}$Lu is problematic especially in certain countries with stringent waste disposal protocols [12]. Assuming that a few μCi of $^{177m}$Lu would be present in a curie of $^{177}$Lu used in a nuclear medicine clinic, the containment and post-decay release of the radioactive waste generated has to be carefully managed by design of appropriate delay tanks. Overall, it can be inferred that direct production of $^{177}$Lu is the most practical route in countries which have access to medium flux research reactors for radioisotope production.

### Complexes of $^{177}$Lu with various bifunctional chelators

Selection of an efficient BFC is essential for preparation of $^{177}$Lu-based radiopharmaceutical. This section describes the coordination chemistry of lutetium and the design concept of BFCs for preparation of $^{177}$Lu-based radiopharmaceuticals. Being the last member of the lanthanide series Lu with 71 electrons has [Xe]$4f^{14}5d^{1}6s^{2}$ configuration. As a result, it loses two outermost 6s electron and the lone 5d electron to generate +3 metal ion species during chemical reaction. As $Lu^{3+}$ species, it has empty s, p, d orbitals and fully filled f orbitals. Since 4f electrons are tightly bound by high effective nuclear charge, they have hardly any contribution to bond formation. Accordingly, coordination between $Lu^{3+}$ ion and the chelator are predominantly electrostatic and governed by the hard and soft acid base (HSAB) principle. Being a hard Lewis acid, $Lu^{3+}$ forms strong complexes with chelators which have high Lewis bases such as carboxylates. Due to lanthanide contraction, $Lu^{3+}$ has the smallest ionic radius (86.1 pm) among the lanthanides. Therefore, because of the high charge density and narrow coordination field, limited number of ligands can be placed around $Lu^{3+}$. Mostly, reciprocal number dictate the coordination number between the ligands without any pertinent effect ascribable to the (s, p, and d) orbitals involved in bond formation.

Chelators for $Lu^{3+}$ are designed based on the following explicit requirements: (i) Labeling efficiency: The process of radiolabeling is performed using a very low-concentration of $^{177}$Lu[$Lu^{3+}$], wherein a high radiolabeling yield is required. Therefore, it is expected that Lu-chelator complexation should be kinetically favored. (ii) In vivo stability: The metal-chelator complex should be insusceptible to hydrolysis under physiological conditions. Additionally, compared to competing proteins, such as human serum albumin (HSA) and transferrin, the chelator should have a higher affinity for Lu [12, 32]. (iii) Metal selectivity: The chelator should have sufficient selectivity towards $^{177}$Lu[$Lu^{3+}$], such that $^{177}$Lu[$Lu^{3+}$] is not replaceable by another metal ions such as $Na^{+}$, $Mg^{2+}$, $K^{+}$, $Ca^{2+}$, $Fe^{2+}$, $Fe^{3+}$, $Co^{2+}$, or $Zn^{2+}$ which co-exist under physiological conditions.

A wide variety of structures have been explored to develop an ideal BFC to satisfy these

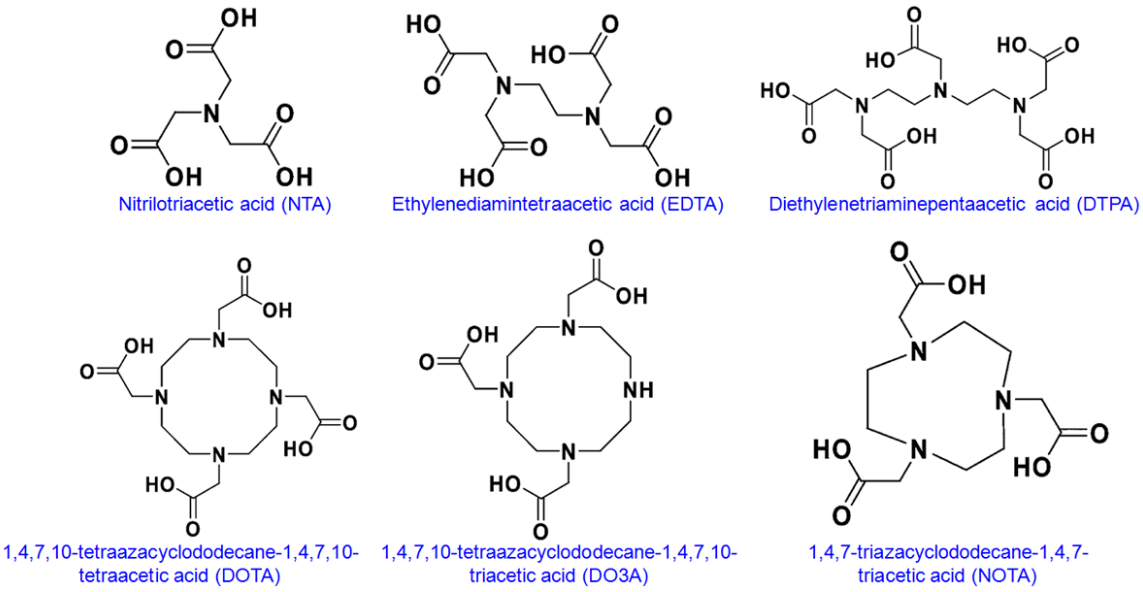


**Figure 4.** Structures of the common bifunctional chelator used for radiolabeling with $^{177}$Lu.

**Table 2.** Commonly used BFCs for $Lu^{3+}$ and log stability constants [12]

| BFC | log stability constant |
|---|---|
| DTPA | 12.5 |
| EDTA | 19.8 |
| NTA | 22.4 |
| DOTA | 25.4 |
| DO3A | 23.0 |
| NOTA | 15.3 |

requirements [8, 12, 33-41]. In fact, $Lu^{3+}$ forms stable complexes with several BFCs and coordination numbers of 6, 7, 8, and 9 have been reported. The common BFCs used for $Lu^{3+}$ are shown in **Figure 4** and their stability constants are summarized in **Table 2**. Among them, DOTA and its derivatives are the most widely used BFCs for preparation of $^{177}$Lu-based radiopharmaceuticals. The DOTA moiety forms the $Na[Lu(DOTA)(H_2O)]_4H_2O$ nine-coordinated complex with high thermodynamic stability and kinetic inertness. The reported $Na[Lu(DOTA)(H_2O)]_4H_2O$ complex has capped square antiprism geometry where the basal plane is occupied by four amine nitrogens of the macrocycle, the capped plane is occupied by four carboxylate oxygens of the carboxylic residues, and the capping position is occupied by a water molecule. In addition to DOTA-based agents, direct radiolabeling of phosphonate analogs of aminocarboxylates, such as ethylenediamine tetra (methylene phosphonic acid) (EDTMP) and 1,4,7,10-tetraazacyclododecane-1,4,7,10-tetramethylene phosphonic acid (DOTMP) have been used for preparation of radiopharmaceuticals for bone pain palliation [42-46]. It is interesting to note that the Lu-aminophosphonate complex (such as Lu-DOTMP) is generally more stable than the Lu-aminocarboxylate complex (such as Lu-DOTA) [12].

For preparation of target specific radiopharmaceuticals, the BFC needs to be conjugated with targeting ligands such as peptides or antibodies. Numerous methods of conjugation are known, among which, the carboxylate or isothiocyanate group in the BFC structure conjugated with the amino group of the targeting ligand, is the approach most widely used [12]. In certain cases, a linker can also be unified between the chelator and the targeting ligand to affect the pharmacokinetics of the radiopharmaceutical [47-49]. These linker groups, such as hydrocarbon chains $(CH_2)_n$, polyethylene glycol (PEG), or polypeptide linkers, can adjust the pharmacokinetics and biodistribution by altering the overall charge and hydrophilicity of the radiopharmaceutical. In all radiolabeling procedures, pH of the reaction mixture plays a crucial role in determining the complexation yield. For DOTA-based chelators, the rate of complex formation increases with increase in pH of the medium. However, at pH >6, $Lu^{3+}$ forms insoluble $Lu(OH)_3$. Therefore,

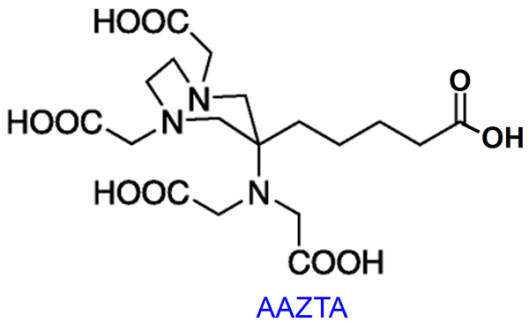


**Figure 5.** Structure of AAZTA chelator.

the optimum pH for radiolabeling is between 5 and 6, and is generally maintained using sodium acetate or ammonium acetate buffers. Interestingly, radiolabeling for DOTMP and EDTMP is done at pH >8, maintained using bicarbonate buffer. This is possible because several folds higher excess of ligand is used compared to $Lu^{3+}$ ions [12]. Only a small fraction of these ligands is radiolabeled and the large excess of the ligands prevent formation of lutetium-hydroxo species through rapid formation of intermediary complexes.

A significant disadvantage of macrocyclic DOTA-based BFCs for preparation of radiopharmaceuticals is the slow rate of complexation with $Lu^{3+}$ ions [12]. Accordingly, heating becomes essential in most radiolabeling processes to increase the kinetics of the chelation process. Generally, heating is performed at 90-95°C for 25-30 min to obtain near quantitative radiolabeling yield [50-52]. This especially becomes a serious challenge when DOTA is conjugated with temperature sensitive biomolecules such as monoclonal antibodies or their engineered fragments. From this perspective, diethylene triamine penta acetic acid (DTPA) based BFCs have been proposed for room temperature radiolabeling with $^{177}$Lu [53-57]. However, some DTPA based complexes are found to dissociate under physiological conditions and release free $Lu^{3+}$ ions *in vivo* [12]. To circumvent this limitation, recently, AAZTA (1,4-bis (carboxymethyl)-6-[bis (carboxymethyl)]amino-6-methylperhydro-1,4-diazepine) based chelators were developed which demonstrated quantitative labeling (>95%) with $^{177}$Lu at room temperature within 5 minutes (**Figure 5**) [58-61]. The complexes demonstrated excellent radiochemical stability and therefore this class of chelators holds promise for development of new generation of $^{177}$Lu-based radiopharmaceuticals.

## Potential $^{177}$Lu-based radiopharmaceuticals in preclinical and clinical settings

A number of $^{177}$Lu-based agents have been prepared using $^{177}$Lu produced by direct neutron activation route in medium flux research reactors, some of which have been translated to the clinic. Targeting ligands such as peptides, monoclonal antibodies and their engineered fragments, phosphonates, small molecules and nanoparticles have been evaluated as potential agents for targeted radiotherapy. An outline of the research efforts that have predicted and established the practicality of $^{177}$Lu produced by direct neutron activation route for potential applications in targeted therapy is given below.

### *Somatostatin receptor targeting agents*

Somatostatin (sst) receptors are typically overexpressed in a variety of tumors of neuroendocrine origin in the pancreas, lung, intestine and thyroid [62, 63]. Over the last two decades, there has been concerted research in the field of sst targeting in oncology for both diagnostic and therapeutic indications [64, 65]. Currently, five subtypes (sst1-sst5) have been identified and cloned, out of which sst2 receptors are predominantly expressed in neuroendocrine tumors (NETs) [66-68]. The presence of sst2 receptors in NETs has opened up the avenue for peptide receptor radionuclide therapy (PRRT). In this regard, $^{177}$Lu labeled sst analog, 1,4,7,10-tetraazacyclododecane-$N^{I}$,$N^{II}$,$N^{III}$,$N^{IIII}$-tetraacetic acid(D)$Tyr_3$-octreotate (DOTATATE) is an established agent in the management of patients with inoperable or metastatic NETs [69-79]. This radiopharmaceutical is able to irradiate tumors and their metastases via internalization through sst2 receptors, generally overexpressed on the cell membrane. This radiopharmaceutical has evolved mainly during the years 2001-2010 and till recently, was the most widely used $^{177}$Lu-labeled agent in clinical context. Nevertheless, significant volume of clinical studies with $^{177}$Lu-DOTATATE have been performed during the last decade using medium specific activity $^{177}$Lu produced by direct neutron activation route, which are summarized below.

The protocol for formulation of clinical dose of $^{177}$Lu-DOTATATE using medium specific activity $^{177}$Lu was optimized by Das et al. [80, 81]. A peptide/metal ratio of ~2 was found to be optimal for complexation wherein radiolabeling yields >95% could be obtained. Subsequently, Mathur et al. performed systematic studies towards bulk scale formulation of "ready-to-use" $^{177}$Lu-DOTATATE in a centralized radiopharmacy [82]. The authors observed that 740 MBq/mL of $^{177}$Lu-DOTATATE formulation with gentisic acid (1.5% w/v) was safe for human use (>98% radiochemical purity) for more than 1 week from the date of production when stored at -70°C. Preliminary clinical studies carried out in NET patients with several batches of $^{177}$Lu-DOTATATE formulation exhibited desired uptake in the tumor and its metastatic sites to obtain the expected therapeutic outcome. This strategy would aid towards widespread deployment of this radiopharmaceutical from centralized radiopharmacy to distant nuclear medicine centers for the maximum benefit of the cancer patients. It is known that the kidneys are the critical organs in PRRT, as the radiopharmaceutical gets cleared from the biological system through the renal route [83, 84]. Consequently, renal function is known to worsen after PRRT. From this perspective, Gupta et al. analyzed the glomerular filtration rate (GFR), increase in serum creatinine (SCr), and changes in hemogram parameters between pretherapy and at least 6 months after last cycle post-therapy with $^{177}$Lu-DOTATATE [84]. It was observed that $^{177}$Lu-DOTATATE therapy led to worsening of renal function revealed by a decline in GFR and increase in SCr. Hematologic toxicity was relatively rare and could be managed as encountered. In this study, the authors analyzed GFR and SCr levels 6 weeks after completion of therapy. However, a long follow up would be required to conclude about the final outcome and toxicity of $^{177}$Lu-DOTATATE therapy. The same group of authors further performed dosimetric analyses of kidneys, liver, spleen, pituitary gland and neuroendocrine tumors of 61 patients treated with $^{177}$Lu-DOTATATE [85]. Favorable biodistribution was observed with $^{177}$Lu-DOTATATE with high affinity to tumors overexpressing sst receptor. The results indicated that highest doses were delivered to the kidneys and spleen with some doses to the liver and pituitary gland. However, there were no serious clinical consequences. It could be concluded that $^{177}$Lu-DOTATATE therapy resulted in high tumor doses with likelihood of injection of up to 40 GBq of cumulative activity in fractions.

In an interesting study, Jois et al. evaluated the feasibility of $^{177}$Lu-DOTATATE therapy in non-$^{131}$I avid metastatic differentiated thyroid carcinoma patients [86]. However, the authors could not arrive at a definite conclusion on the therapeutic efficacy of $^{177}$Lu-DOTATATE in the studied group of patients and further studies would be required. Basu et al. demonstrated that metastatic Merkel cell carcinoma patients responded favorably to targeted therapy with $^{177}$Lu-DOTATATE [87]. The authors inferred that considering the relative well tolerability, minimal side-effects and specificity of the treatment, $^{177}$Lu-DOTATATE therapy could evolve as the first line therapy in patients of metastatic Merkel cell carcinoma. Nevertheless, further examination in a greater number of patients would be required in the future. From study in a large number of patients over a period of 5 years, Danthala et al. showed that $^{177}$Lu-DOTATATE therapy could be considered irrespective of prior chemotherapy, surgery or extent of disease [88]. The dose delivered was primarily responsible for treatment response and progression free survival and the best results were obtained when more than two cycles of $^{177}$Lu-DOTATATE therapy were given, with cautious monitoring of the likely side effects. The follow up imaging in a typical responding patient after four cycles of $^{177}$Lu-DOTATATE therapy is shown in **Figure 6**. In another similar study, Ballal et al. evaluated the outcome, toxicity, survival, and quality of life after concomitant $^{177}$Lu-DOTATATE and Capecitabine therapy in large number of patients with advanced neuroendocrine tumor [89]. The authors observed that concomitant $^{177}$Lu-DOTATATE and Capecitabine therapy was highly effective, delayed the time to progression, and improved the overall survival in patients with metastatic neuroendocrine tumors. Life-threatening toxicity was not reported in any of the patients. Overall, this combined therapeutic modality can be applicable in selective patients with aggressive disease where the primary goal is not to achieve complete resolution of the diseases, but rather to arrest disease progression. Similar results were also reported by Yadav et al. in patients

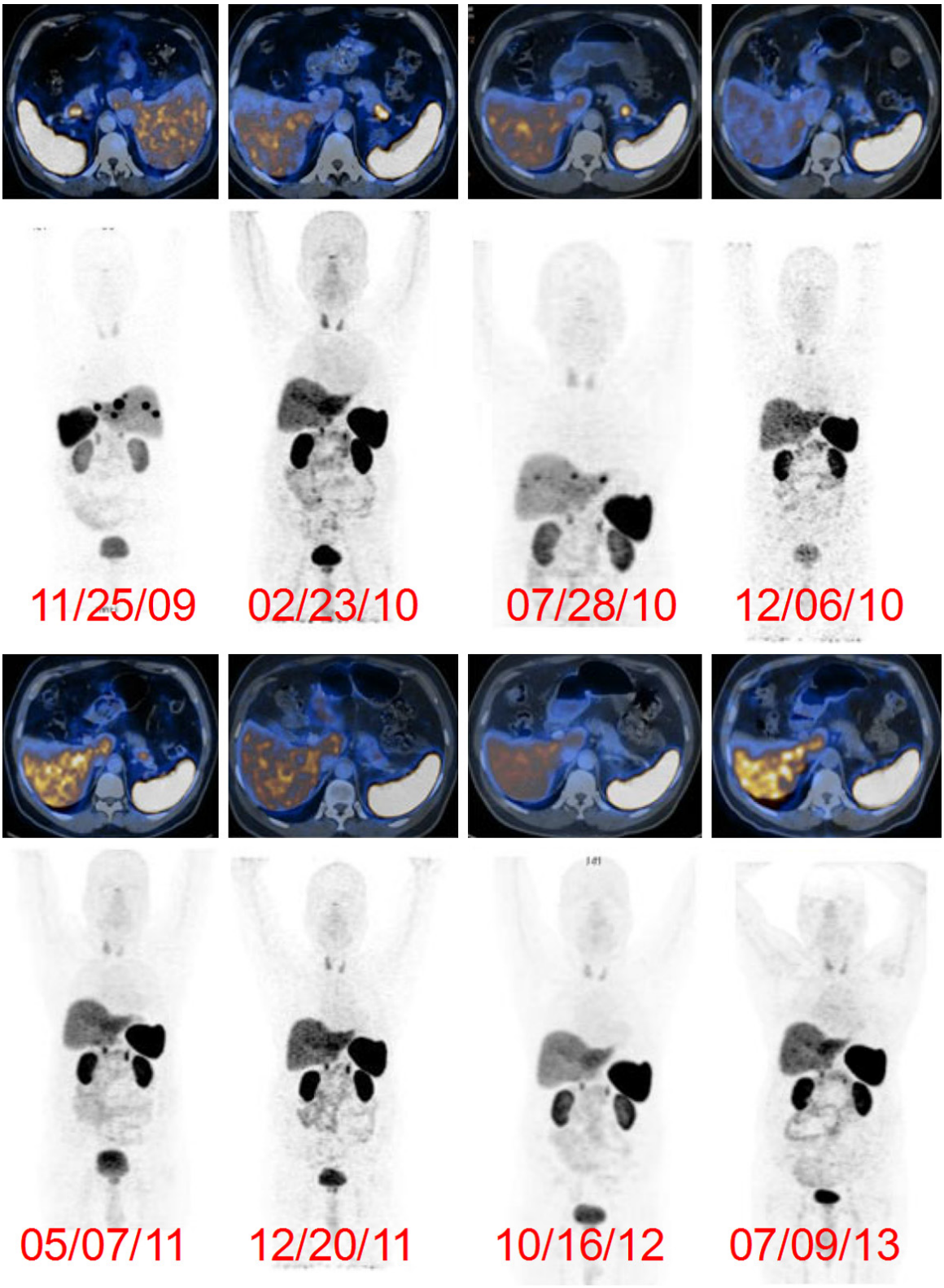


**Figure 6.** Post-therapy, $^{68}$Ga-DOTA-NOC PET scans in a 57-year-old man with pancreatic neuroendocrine tumor with extensive liver metastases. The patient was treated with four cycles of $^{177}$Lu-DOTATATE and on regular follow-up showed significant decreases in both the primary tumor in the pancreas and hepatic metastases. Adapted from Ref [88].

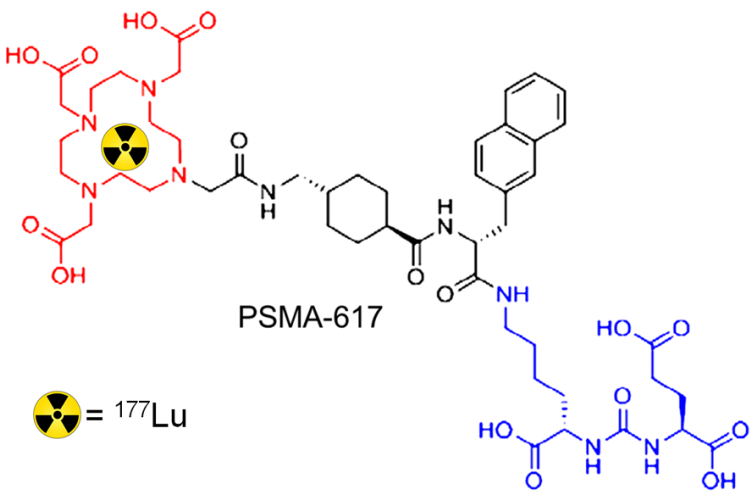


**Figure 7.** Structure of PSMA-617.

with malignant paragangliomas [90]. In the recent times, numerous clinical studies have been reported which demonstrated the efficacy of $^{177}$Lu-DOTATATE therapy in metastatic neuroendocrine tumors [91-102]. In future, multi-institutional randomized clinical trials would be desirable to further establish the safety and clinical efficacy of this treatment modality in a large number of patients.

*Prostate specific membrane antigen inhibitor*

Prostate cancer is among the most common malignancies in men globally, with 10-20% of the cases progressing to metastatic castration resistant prostate cancer (mCRPC) [103, 104]. Approximately, 90% of mCRPC patients present with bone metastases causing severe pain, stress fractures, poor quality of life and morbidity [104]. A variety of therapeutic procedures such as chemotherapy, androgen deprivation therapy and immunotherapy have conventionally been proposed in the treatment of mCRPC. However, very few therapeutic options are available for the patients who have the disease that progresses with steadily increasing serum prostate specific antigen (PSA) level. Especially for such patients, prostate specific membrane antigen (PSMA), a type II transmembrane glycoprotein overexpressed in prostate cancer, is an excellent target in the imaging and therapy of mCRPC [105, 106]. Several urea based peptidomimmetic agents have been reported for targeting PSMA, out of which the commercially available PSMA-617 has received widespread attention for radiolabeling with $^{177}$Lu [105, 106]. The structure of PSMA-617 is shown in **Figure 7**. In fact, $^{177}$Lu-PSMA-617 therapy which evolved within a very short span of time in the last decade has revolutionized the radionuclide therapy of mCRPC [107-116]. The growth of this radiopharmaceutical has been so rapid and huge that it has overtaken $^{177}$Lu-DOTATATE as the most widely used $^{177}$Lu-based radiopharmaceutical in clinical context.

Utilizing medium specific activity $^{177}$Lu produced by direct neutron activation route in medium flux research reactor, our group was among the first to report the protocol for formulation of therapeutic dose (7.4 GBq) of $^{177}$Lu-PSMA-617 in a hospital radiopharmacy [117]. Preliminary clinical studies were performed in five patients with biopsy proven mCRPC. *In vivo* SPECT imaging post administration of therapeutic dose showed specific targeting of the radiopharmaceutical in the lesion sites and similar biodistribution pattern as in diagnostic $^{68}$Ga-PSMA-11 PET scans performed earlier. Clinical investigations conducted after therapy did not show any adversative side effects in any of the five patients and also there was significant reduction in PSA levels in the five patients demonstrating the preliminary efficacy of the therapeutic procedure. This work was further extended to scale-up the procedure for formulation of $^{177}$Lu-PSMA-617 in a centralized radiopharmacy [118]. The protocol was optimized for multidose formulation (>40 GBq) of ready-to-use $^{177}$Lu-PSMA-617 which met the requirements for clinical use and could be shipped to nuclear medicine centers for administration up to 4 days from the date of formulation. These procedures would aid toward widespread utilization of medium specific activity $^{177}$Lu in prostate cancer therapy especially in the developing countries.

To determine the safe activity of $^{177}$Lu-PSMA-617 that can be administered to prevent hematological, liver and renal toxicity, Yadav et al. studied the pharmacokinetics and dosimetry of the radiopharmaceuticals in 26 patients with mCRPC [119]. The mean administered

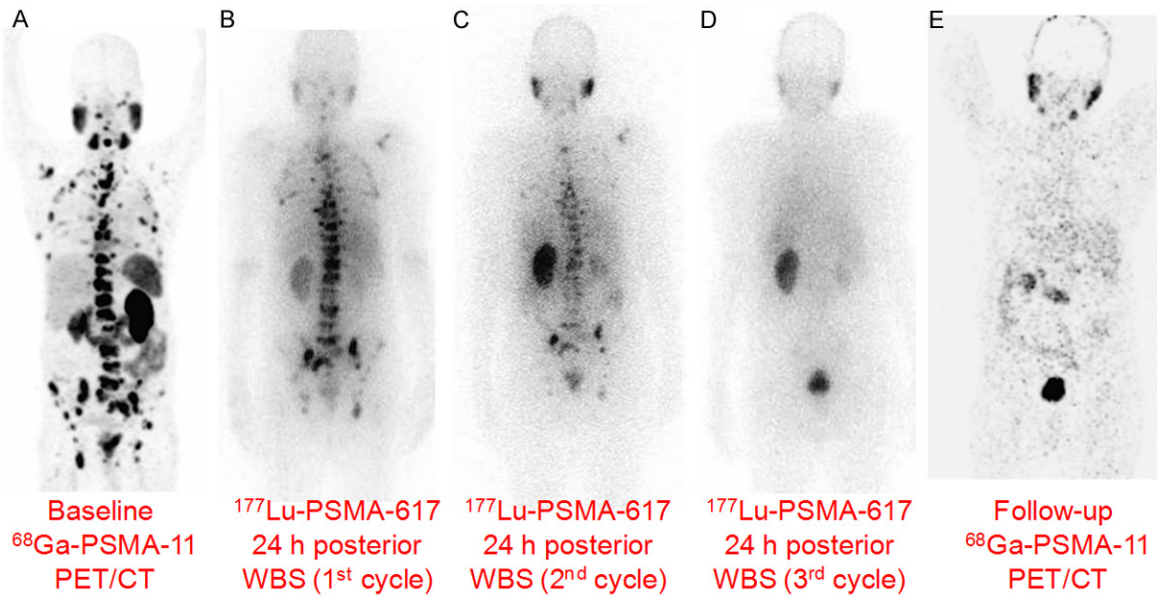


**Figure 8.** $^{177}$Lu-PSMA-617 therapy in a 65-year-old man with mCRPC. (A) The baseline pre-therapy diagnostic $^{68}$Ga-PSMA-11 PET/CT showed PSMA-avid extensive skeletal metastases, (B) Posterior whole body scintigraphy (WBS) 24 h after administration of first cycle of $^{177}$Lu-PSMA-617, (C) Posterior WBS 24 h after administration of second cycle of $^{177}$Lu-PSMA-617 showed remarkable reduction in uptake, (D) Posterior WBS 24 h after administration of third cycle of $^{177}$Lu-PSMA-617 did not show any abnormal uptake, (E) After three cycles of therapy, the follow-up diagnostic $^{68}$Ga-PSMA-11 PET/CT scan showed near complete metabolic response with resolution of the PSMA-avid metastases. Adapted from Ref [120].

activity in the overall population was 2.52±1.3 GBq. Normal physiological uptakes were observed in the lacrimal glands, salivary glands (parotid glands and submandibular glands), liver, spleen, kidneys, intestines and urinary bladder in all the patients. It was observed that the organs with the highest absorbed doses were the salivary glands, followed by the kidneys, receiving 1.24±0.26 and 0.99±0.31 mGy/MBq, respectively. The mean absorbed doses to the liver, urinary bladder and red marrow were 0.36±0.10, 0.243±0.09 and 0.048±0.05 mGy/MBq, respectively. The mean whole-body dose was 0.016±0.003 mGy/MBq. From the point of view of radiation dosimetry, it could be concluded that $^{177}$Lu-PSMA-617 is a safe option for treatment in mCRPC patients. The same group of authors further studied the safety and efficacy of $^{177}$Lu-PSMA-617 in 31 mCRPC patients (age range: 38-81 years) [120]. All the patients underwent $^{68}$Ga-PSMA-11 PET/CT scan prior to inclusion for therapy and were administered with 5069±1845 MBq dose of $^{177}$Lu-PSMA-617 ranging from one to four cycles. Standard physiological uptake of $^{177}$Lu-PSMA-617 occurred in the lacrimal glands, salivary glands, liver, intestines, spleen, kidneys, and bladder (**Figure 8**). In typical patients with complete remission, the mean $SUV_{max}$ of the tumor lesions reduced from 32.67 to 0.38 after $^{177}$Lu-PSMA-617 therapy (**Figure 8**). Further, the authors observed biochemical response in 70.9% (22/31) and clinical response in 67.7% (21/31) patients. Serious life-threatening toxicity was not observed in any of the 31 patients. It was a concluded that $^{177}$Lu-PSMA-617 therapy is a simple and effective procedure with no significant adverse effects and improves the quality of life of end stage mCRPC patients. Similar clinical outcomes were observed in another study reported by Suman et al. [121]. However, these studies need to be performed in larger number of patients who need to be followed up for an extended period of time to arrive at a definitive conclusion. Recently, Adnan and Basu studied the imaging characteristics, peculiarities and response to $^{177}$Lu-PSMA-617 therapy in patients with urinary bladder metastasis by prostate cancer in accordance with Gleason score and dual tracer ($^{68}$Ga-PSMA-11 and $^{18}$F-FDG) PET study [122]. The authors inferred that $^{18}$F-FDG PET/CT along with $^{68}$Ga-PSMA-11 PET/CT, preferably at the

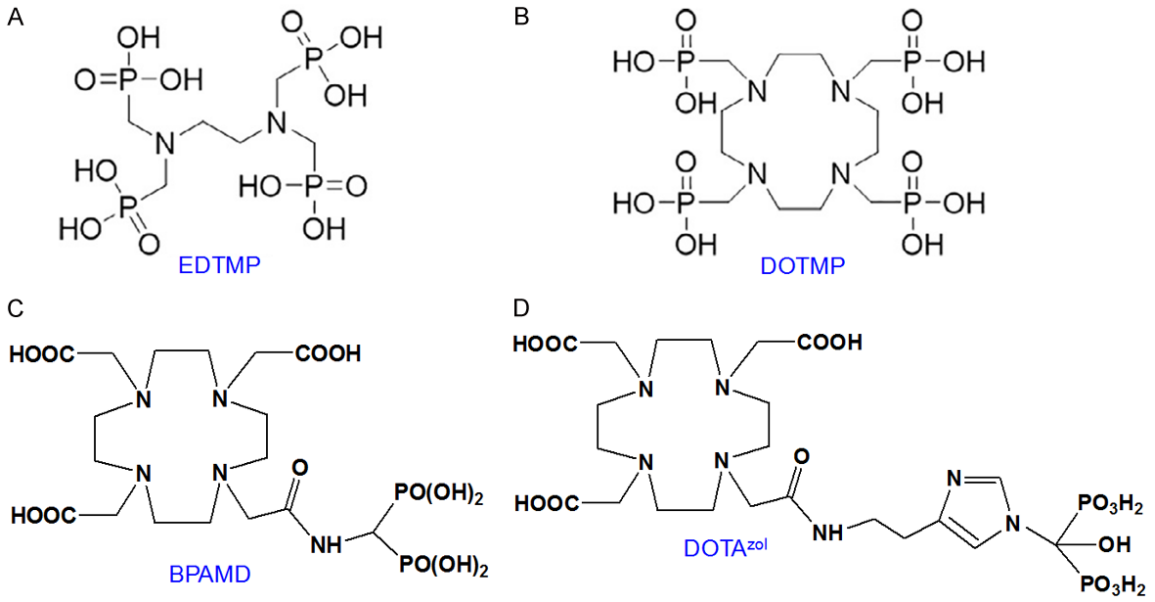


**Figure 9.** Structures of (A) EDTMP, (B) DOTMP, (C) BPAMD and (D) DOTA$^{zol}$.

baseline, can promote prognostic and predictive implications in therapy of mCRPC using $^{177}$Lu-PSMA-617. The major limitation of this study was that it was conducted on just 3 patients and therefore, future studies in larger number of patients would be a worthwhile exercise.

*Bone pain palliation agents*

Bone is one of the common sites of metastases from various types of cancers, which include that of prostate, breast, lung, kidney, bladder, thyroid, lymphomas and sarcomas [123-128]. Of these, primary cancers of prostate, breast and lung account for >80% cases of bone metastases. These metastatic lesions on bone surface have huge impact in the quality of life of those patients, causing complications such as severe bone pain, pathologic fractures, hypercalcemia, and spinal cord compression [129]. The management of bone pain involves a multidisciplinary approach involving systemic and nonsystemic treatments. However, many treatment options have limitations in their efficacy and duration. Some of them manifest significant adverse effects that seriously compromise the quality of life of the cancer patients. Over the last few decades, radiopharmaceuticals are being used widely as an alternate method for palliative care of metastatic bone pain [43, 129-135]. In this regard, EDTMP and DOTMP (**Figure 9A** and **9B**) labeled with $^{177}$Lu have been clinically established as effective radiopharmaceuticals for bone pain palliation [42, 45]. Though these radiopharmaceuticals were developed at the beginning of this century, significant progress took place in the clinical evolution of these radiopharmaceuticals over the last decade and hence dealt in here. Few other bone-targeting $^{177}$Lu-based radiopharmaceuticals have been developed and used in clinical settings over the last decade, a summary of which is provided in **Table 3**.

Using $^{177}$Lu produced via direct neutron activation route, the results of Phase 0/I study dealing with the pharmacokinetics, dosimetry and toxicity analysis of $^{177}$Lu-EDTMP in patients was first reported by Bal et al. [136]. In this study, the authors assessed the biokinetics of skeletal and non-skeletal uptake of $^{177}$Lu-EDTMP (172.7-206.9 MBq) in 6 different patients with metastatic prostate cancer. The authors obtained the data of whole skeletal uptake, blood and fractionated urine samples and performed dosimetric calculations. Prolonged retention of activity in bone was observed in all the patients. It was observed that excretion took place mainly through renal route and blood clearance was rapid and biphasic. The mean estimated dose to the red marrow was 0.8±0.15 mGy/MBq while the mean total body

**Table 3.** Bone targeting $^{177}$Lu-based radiopharmaceuticals used in clinical context

| Formulation | Type of study | Total population | Clinical outcome | Ref. |
|---|---|---|---|---|
| $^{177}$Lu-EDTMP | Phase 0 | 6 patients with metastatic prostate cancer | $^{177}$Lu-EDTMP has excellent pharmacokinetic and dosimetric properties, besides being safe and effective. | [136] |
| | Phase I | 21 patients with metastatic prostate cancer | | |
| | Phase II | 44 patients with documented breast carcinoma (12 patients) or castration-resistant prostate carcinoma (32 patients) and skeletal metastases | $^{177}$Lu-EDTMP was found to be a safe and effective radiopharmaceutical for bone pain palliation in patients with metastatic prostate and breast carcinoma. There were no differences in efficacy or toxicity between patients receiving low-dose and high-dose $^{177}$Lu-EDTMP. | [137] |
| $^{177}$Lu-DOTMP | Preliminary clinical investigation | 5 male patients with metastatic prostate cancer or lung cancer | Desired human pharmacokinetic features, namely, preferential localization of $^{177}$Lu-DOTMP in skeletal lesion sites and almost no uptake in soft tissue or any other major nontarget organ was observed. Also, reduction of pain and almost no adverse side effects in patients was exhibited. | [44] |
| | Systematic clinical investigation in larger cohort of patients | 27 male patients with histologically proven carcinoma and painful widespread skeletal metastases | $^{177}$Lu-DOTMP is an effective treatment option for immediate bone pain palliation with improvement in quality of life. The notable adverse effects were transient mild-moderate hematotoxicity and was well-tolerated by all the patients. | [141] |
| $^{177}$Lu-BPAMD | Preliminary clinical investigation | 2 patients with metastatic prostate cancer | Significant reduction in pain after 1 week without any adverse effect. | [149] |
| $^{177}$Lu-DOTA$^{zol}$ | Systematic clinical investigation | 40 patients with metastatic prostate, breast or lung cancer | According to the visual analogue score (VAS) criteria, complete, partial, and minimal responses were observed in 11 (27.5%), 20 (50%), and 5 patients (12.5%), respectively with an overall response rate of 90% with 27.5% of complete response and 50% of partial response. Overall, $^{177}$Lu-DOTA$^{zol}$ is an ideal, safe and effective agent in the treatment of metastatic bone pain. | [157] |

dose was 0.16±0.04 mGy/MBq. A maximum tolerated dose (MTD) of 2000-3250 MBq for $^{177}$Lu-EDTMP was calculated. For the phase I study, therapeutic dose (692-5550 MBq) of $^{177}$Lu-EDTMP was administered in patients with metastatic prostate cancer. The toxicity of the dose was evaluated by assessment of hemoglobin levels, platelet and leukocyte counts over 12 weeks. Out of the 21 patients, transient toxicity was observed in 14 patients of whom 6 had baseline toxicity. Grade 3-4 toxicity was manifested in significantly higher number of patients beyond the MTD. Visual analog scale (VAS) score was used for analyzing the pain relief and it was found that 86% of the patients got relief within the period of 7 weeks. Based on these results, the authors concluded that $^{177}$Lu-EDTMP not only has excellent pharmacokinetic and dosimetric characteristics but is also safe and effective. The study was extended by the same group of authors, wherein they conducted Phase II study with $^{177}$Lu-EDTMP in patients with breast and prostate cancer [137]. In this study also, the radiopharmaceutical was found to be safe and efficacious. There was no difference in toxicity or efficacy between patients receiving low and high doses of $^{177}$Lu-EDTMP.

In another interesting study, Thapa et al. compared $^{177}$Lu-EDTMP with United States Food and Drug Administration (US FDA) approved agent, $^{153}$Sm-EDTMP in patients with skeletal metastases due to primary cancer [138]. The patients were divided into two groups: one group was administered with $^{177}$Lu-EDTMP and the other group was administered with $^{153}$Sm-EDTMP. Doses of both the radiopharmaceuticals were maintained at 37 MBq/kg of body weight. Analgesic, pain, quality of life scores and bone proliferation marker were used to examine efficacy. From this study, the authors could conclude that $^{177}$Lu-EDTMP has pain response efficacy similar to that of $^{153}$Sm-EDTMP, coupled with minimal side effects and improved quality of life. Overall, $^{177}$Lu-EDTMP is a safe alternative to $^{153}$Sm-EDTMP and in view of relatively longer half-life of $^{177}$Lu, $^{177}$Lu-EDTMP is especially advantageous for centers having no nearby access to $^{153}$Sm-EDTMP. A similar clinical study was later reported by Sharma et al., where the authors highlighted that both $^{177}$Lu-EDTMP and $^{153}$Sm-EDTMP offered competitive efficacy for palliative care of metastatic bone pain and can be interchangeably used as per the availability [139].

Comparative studies of $^{177}$Lu-EDTMP with its macrocyclic analog $^{177}$Lu-DOTMP in preclinical settings established that $^{177}$Lu-EDTMP has marginally higher skeletal accumulation in

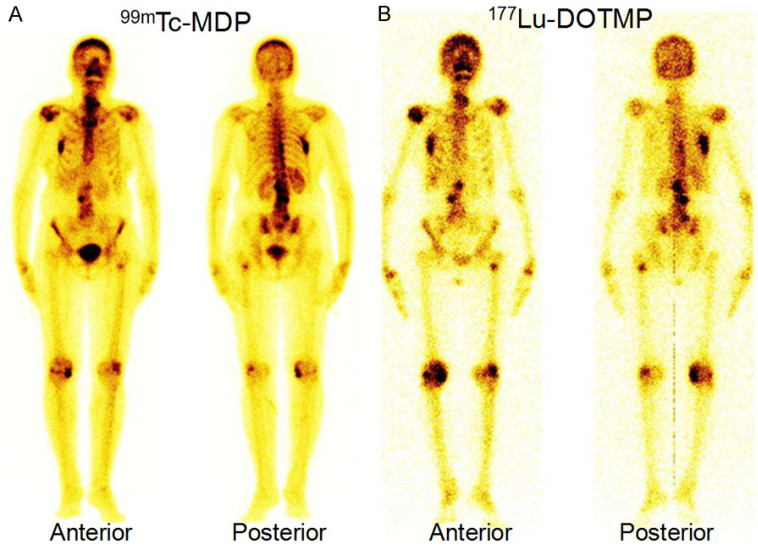


**Figure 10.** Anterior and posterior images from (A) $^{99m}$Tc-MDP WBS of a 55-year-old woman with breast cancer showing widespread skeletal metastases, (B) $^{177}$Lu-DOTMP post-therapy images showing uptake pattern similar to that of $^{99m}$Tc-MDP bone scan.

comparison to that of $^{177}$Lu-DOTMP, while the latter showed slightly faster blood clearance along with lower retention in liver and kidneys [140]. Also, $^{177}$Lu-DOTMP demonstrates superior kinetic robustness compared to $^{177}$Lu-EDTMP. Our group has developed a robust and easily adaptable protocol for formulation of clinically relevant dose of $^{177}$Lu-DOTMP in a hospital radiopharmacy [44]. The radiolabeled formulation demonstrated excellent in vitro stability and desired pharmacokinetics in preclinical settings. Preliminary clinical investigations were carried out in limited number of patients which showed specific skeletal accumulation with preferential localization in the metastatic lesion sites and almost no uptake in soft tissue or any other major non-target organ (**Figure 10**). Pain reduction was observed in all the patients 1 week after therapy. Recently, investigation in a larger cohort of patients was carried out by us to infer on the clinical efficacy and safety of the radiopharmaceutical [141]. In this study, 27 patients with painful skeletal metastases were administered with 37 MBq/kg dose of $^{177}$Lu-DOTMP. Overall response was seen in 77.8% of patients with significant improvement in median VAS and mean analgesic score (AS) at 2 months post-therapy. Best response was seen in patients with breast cancer (100%) followed by prostate cancer (81%) and lung cancer (28%). Improvement in quality of life was noted in 40% of patients. However, grade 2/3 anaemia, grade 1/2 leukopenia and grade 1/3 thrombocytopenia were seen in 37%, 11.1%, and 18.5% patients, respectively in the follow-up. It could be inferred that $^{177}$Lu-DOTMP was an effective treatment option for bone pain palliation and led to improvement in quality of life. The radiopharmaceutical appeared to be safe with mild to moderate hematotoxicity which was well tolerated by the patients. Nevertheless, controlled studies with larger sample size are warranted for better evaluation of the overall survival of the patients.

A strategy which has recently evolved is to form well-defined and highly stable complex by keeping the bisphosphonate moiety out of the radiometal chelating framework and using the conventional bifunctional chelating approach for complexation with $^{177}$Lu [142-148]. In this regard, a new macrocyclic bisphosphonate [4-{[bis-(phosphonomethyl))carbamoyl]methyl}-7,10-bis(car-boxymethyl)-1,4,7,10-tetraazacyclododec-1-yl)acetic acid)] (BPAMD) has been developed which guarantees $^{177}$Lu-complexation with high thermodynamic stability and appreciable kinetic rigidity *in vivo* (**Figure 9C**) [145, 146]. Consequently, BPAMD concentration in the radiopharmaceutical could be significantly lowered which aided towards targeting micrometastatic sites, resulting in enhanced therapeutic efficacy. Our group has developed a protocol for formulation of therapeutically relevant dose of $^{177}$Lu-BPAMD using medium specific activity $^{177}$Lu produced by direct $^{176}$Lu (n,γ) $^{177}$Lu reaction [149]. After establishing the efficacy of the product in preclinical settings, preliminary clinical investigations were carried out in limited number of patients with metastatic bone pain. Intense uptake of the radiopharmaceutical was observed in the metastatic skeletal lesions with insignificant uptake in any other major non-targeted organs. In all the patients, considerable reduction in pain was observed after one week without any adverse effects.

Despite promising clinical results obtained in palliative radiotherapy using $^{177}$Lu-BPAMD,

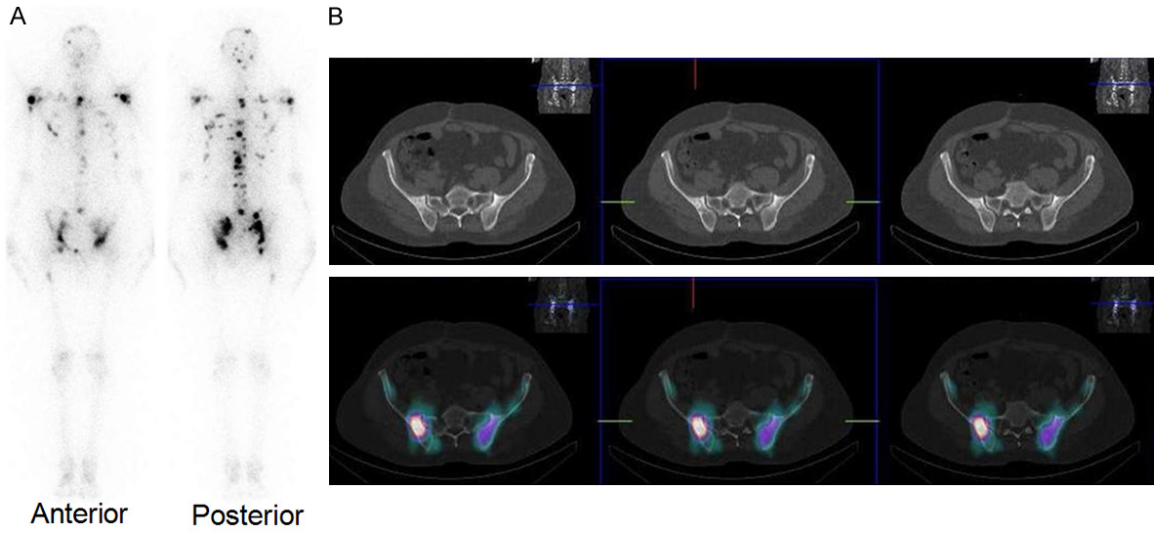


**Figure 11.** A 55-year-old male diagnosed with prostatic adenocarcinoma was administered with $^{177}$Lu-DOTA$^{zol}$. (A) Post-therapy WBS 24 h post-administration showed uptake in multiple skeletal sites, (B) Post-therapy SPECT/CT showed uptake in the pelvic bone metastases. Adapted from Ref [157].

there is still much potential for improvement with regard to further enhancement of accumulation of the radiolabeled agent in bone metastases and minimizing the uptake in non-targeted organs. In this regard, the side chains on the central carbon atom of the bisphosphonate moiety play a significant role in the bisphosphonate's activity, i.e., in terms of affinity to hydroxyapatite (the constituent of bone). Higher bone accumulation can be observed using a hydroxybisphosphonate because of increased affinity for hydroxyapatite [150]. Furthermore, an aromatic nitrogen atom in the side chain could cause building of another hydrogen bond and thereby also raise bone accumulation [146, 151]. One such bisphosphonate is zoledronic acid, which has also been found to influence biochemical processes. These molecules possess an inhibiting effect on the farnesyl diphosphate synthase (FPPS) and inhibition of this enzyme causes an increased apoptosis rate [146, 151]. Taking these factors into consideration, a DOTA-conjugated zoledronate (DOTA$^{zol}$, **Figure 9D**) was synthesized and labeled with $^{68}$Ga and $^{177}$Lu and examined in *in vitro* and *ex vivo* biodistribution studies, as well as small animal PET and SPECT studies [152-156]. Recently, Yadav et al. evaluated the safety and efficacy of $^{177}$Lu-DOTA$^{zol}$ as bone pain palliation agent in 40 patients suffering from bone metastasis due to variety of cancers [157]. The patients were treated with either 1 or 2 cycles of $^{177}$Lu-DOTA$^{zol}$. The biodistribution and uptake of $^{177}$Lu-DOTA$^{zol}$ in a patient with skeletal metastases from prostate cancer is shown in **Figure 11**. According to the VAS response assessment criteria, complete, partial, and minimal responses were observed in 11 (27.5%), 20 (50%), and 5 patients (12.5%), respectively with an overall response rate of 90%. Though this was a non-randomized clinical study, the promising results obtained herein amply demonstrated that $^{177}$Lu-DOTA$^{zol}$ is an ideal, safe and effective agent in the treatment of metastatic bone pain.

*Integrin $\alpha_v\beta_3$ targeting agents*

Integrin $\alpha_v\beta_3$, which is a receptor for the extracellular matrix proteins with the exposed arginine(R)-glycine(G)-aspartic acid(D) tripeptide sequence, plays an important role in angiogenesis during tumor growth and metastasis. For both early detection as well as treatment of rapidly growing solid tumors, the overexpression of integrin $\alpha_v\beta_3$ presents an interesting molecular target The preparation and biological evaluation of $^{177}$Lu-labeled cyclic RGD peptide dimer E[c(RGDfK)]$_2$ (E = glutamic acid) coupled with DOTA (1,4,7,10-tetraazacyclododecane-1,4,710-tetraacetic acid) [$^{177}$Lu-DOTA-E[c(RGDfK)]$_2$] in BALB/c bearing human glioblastoma (U87MG) xenograft was reported by Shi et al. [158] and Luna-Gutierrez et al.

[159]. The radiotracer demonstrated specific uptake in the tumor. Realizing the scope of this agent for future clinical investigation, our group optimized the protocol for formulation of clinically relevant doses of $^{177}$Lu-DOTA-E[c(RGDfK)]$_2$ using medium specific activity $^{177}$Lu produced via direct neutron activation route [160]. In this study, a therapeutic dose (7.4 GBq) of the radiolabeled agent was formulated in ~63 GBq/μM specific activity with high yield (98.2±0.7%) and appreciable *in vitro* stability. Biodistribution studies carried out in C57BL/6 mice bearing melanoma tumors revealed specific accumulation of the radiolabeled conjugate in tumor (3.80±0.55% ID/g at 30 min p.i.) with high tumor-to-blood and tumor-to-muscle ratios. This reported protocol could be followed to prepare clinical dose of the radiolabeled agent in a hospital radiopharmacy.

In a latest development, Parihar et al. demonstrated the utility of $^{177}$Lu-DOTA-E[c(RGDfK)]$_2$ in treatment of patients with differentiated thyroid carcinoma and presenting with thyroglobulin elevation with negative $^{131}$I scintigraphy (TENIS) [161]. In fact, TENIS in thyroid cancer patients causes a serious management challenge due to limited treatment modalities. Recently, RGD peptides have been identified as effective agents for this purpose due to overexpression of integrin $\alpha_v\beta_3$ in differentiated thyroid cancer [161]. The authors reported the case of a 54-year-old female patient with papillary thyroid cancer who developed TENIS syndrome after receiving 500 GBq of $^{131}$I in cumulative doses. The patient experienced considerable adverse effects with hardly any clinical improvement on sorafenib therapy for 1 year. She also presented with severe pain and a palpable hard mass in the pre-sternal region. After $^{68}$Ga-DOTA-E[c(RGDfK)]$_2$ PET/CT scan for evaluating the extent of the disease and pre-therapy assessment, she was administered with 5.5 GBq of $^{177}$Lu-DOTA-E[c(RGDfK)]$_2$ (**Figure 12**). Post-therapy follow-up showed significant pain relief and reduced pre-sternal swelling, suggesting clinical benefit. At 4 months post-therapy, $^{68}$Ga-DOTA-E[c(RGDfK)]$_2$ PET/CT scan showed reduced uptake in the cancerous lesions indicating clinical benefit (**Figure 12**). Though the results of this preliminary clinical study are quite promising, randomized clinical trials in large cohort of patients are warranted to understand the real benefits of this approach.

*Monoclonal antibodies*

Over the last several years, radiolabeled monoclonal antibodies are being increasingly used for personalized management of various types of cancers [54, 162-166]. Lutetium-177 is an important radioisotope in this regard as its relatively long half-life matches the pharmacokinetics of the antibodies. Our group had reported the formulation of clinically relevant doses of $^{177}$Lu-labeled cetuximab using low specific activity $^{177}$Lu and demonstrated its efficacy in preclinical settings [167]. Subsequently, in order to improve the pharmacokinetics, Fab fragments of cetuximab were generated by papain digestion and used for radiolabeling with $^{177}$Lu for formulation of therapeutically relevant doses [168]. The promising results obtained in these studies might expedite the process of formulation of large doses of $^{177}$Lu-labeled immunoconjugates in clinical settings for the benefit of the cancer patients. In a recent preclinical study, a CD38 targeting monoclonal antibody (daratumumab) was radiolabeled with $^{89}$Zr and $^{177}$Lu for potential theranostic applications [169]. The results suggested that CD38 is a lymphoma specific marker, meriting further exploration in clinical context. The authors reported high and persistent tumor uptake and significant tumor inhibition with radiolabeled daratumumab for the theranostic of CD38-positive cancer in mice model. Histological and hematological analyses established negligible toxicity of $^{177}$Lu-labeled daratumumab in mice model. It was inferred that further advancement of this strategy would aid significantly in lymphoma patient stratification and management.

The first clinical study with $^{177}$Lu-labeled monoclonal antibody using low specific activity $^{177}$Lu was reported by Yadav et al., wherein the authors studied the dosimetry of $^{177}$Lu-DOTA-rituximab in 10 patients with relapsed/refractory non-Hodgkin's lymphoma [170]. In this study, rituximab (375 mg/m$^2$), followed by 1.85 GBq of $^{177}$Lu-DOTA-rituximab was administered as a slow intravenous infusion and SPECT images were acquired and internal dose estimation was performed using OLINDA software. The authors determined that the effective half-life of $^{177}$Lu-DOTA-rituximab was 100±28 h and

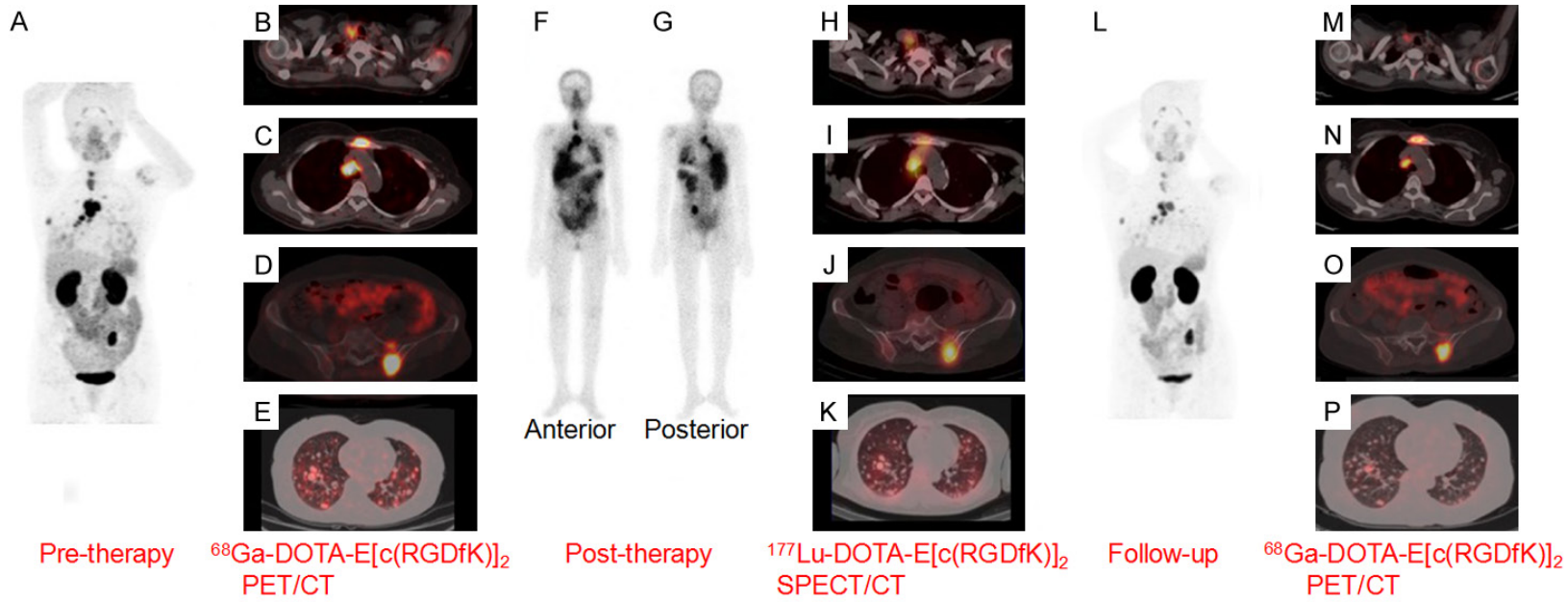


**Figure 12.** A 54-year-old woman with papillary thyroid carcinoma who developed TENIS syndrome after receiving 500 GBq of $^{131}$I in cumulative doses, was administered with $^{177}$Lu-DOTA-E[(cRGDfK)$_2$] therapy. $^{68}$Ga-DOTA-E[(cRGDfK)$_2$] PET/CT was performed to evaluate disease extent and for pre-therapy assessment. (A) Pre-therapy, the maximum intensity projection (MIP) image with $^{68}$Ga-DOTA-E[(cRGDfK)$_2$] PET scan, transaxial fused PET/CT images showed increased tracer uptake in the (B) thyroid remnant, (C) cervical lymph nodes (D) mediastinal lymph node, lytic skeletal lesions with soft tissue component in the sternum and left iliac bone, (E) multiple lung nodules. Post-therapy WBS in (F) anterior and (G) posterior views revealing the overall distribution of $^{177}$Lu-DOTA-E[(cRGDfK)$_2$] and transaxial fused SPECT/CT images (H-K) showing tracer uptake at sites corresponding to $^{68}$Ga-DOTA- E[(cRGDfK)$_2$] -avid lesions. (L) Post-therapy follow-up $^{68}$Ga-DOTA- E[(cRGDfK)$_2$] PET/CT MIP image and transaxial fused PET/CT images showed tracer uptake in the (M) thyroid remnant with cervical lymph nodes, (N) mediastinal lymph node, lytic skeletal lesions with significant reduction in soft tissue component in the sternum, (O) left iliac bone and (P) multiple lung nodules, suggesting response to therapy. Adapted from Ref [161].

the critical organ in their study was the red marrow. The average total body dose, effective dose, and effective dose equivalent calculated in all 10 patients were 0.13±0.02, 0.15±0.03, and 0.22±0.04 mGy/MBq, respectively. A major limitation of this study was the lack of generalization or extrapolation of doses in the clinical setting. Hence, patient specific dosimetry is warranted in a larger cohort of patients to get rid of the variations and reduce the possibility of dose-limiting toxicity. In another study, Bhusari et al. formulated clinically relevant doses of $^{177}$Lu-DOTA-trastuzumab and performed feasibility of radioimmunotherapy assessment in breast cancer patients [171]. The patient studies showed the localization of $^{177}$Lu-DOTA-trastuzumab at primary as well as metastatic sites (HER2 positive) in the planar and SPECT/CT images (**Figure 13**). No tracer uptake was observed in HER2 negative patients that indicated the specificity of the radioimmunoconjugate (**Figure 13**). Despite promising results, more clinical studies need to be performed with escalating trastuzumab doses and dosimetric evaluation to determine the therapeutic index of $^{177}$Lu-DOTA-trastuzumab.

*Radiation synovectomy agents*

In radiation synovectomy, beta-emitting radionuclides in colloidal or particulate form (1-10 μm size range) are intraarticularly injected into the affected synovial joints. This is an effective treatment modality in patients suffering from inflammatory-rheumatoid and degenerative joint diseases [172-180]. In this treatment modality, the uptake of radionuclides occurs in the synovial lining cells, phagocytized by the outermost cellular layer of the synovial membrane and deliver radiation dose to the synovium without excessive irradiation of surrounding tissue. Owing to its favorable nuclear decay characteristics, cost-effective availability and ease of production, medium specific activity $^{177}$Lu is an appealing radioisotope for preparation of radiation synovectomy agents. For the first time, our group reported a kit-based strategy for expedient formulation of ~400 MBq dose of $^{177}$Lu-labeled hydroxyapatite ($^{177}$Lu-HA) particles at hospital radiopharmacy and its clinical investigations in patients with rheumatoid arthritis of knee joints [181, 182]. Significant improvement in disease condition was observed in all the patients within 15 days post-therapy. No significant onset of pain was observed within 30 days post-therapy. Similar results were obtained on administration of $^{177}$Lu-HA in patients with rheumatoid arthritis of wrist joints (**Figure 14**). Despite encouraging results, clinical studies on larger number of patients and pain response over a longer period of time are warranted to understand the efficacy of this treatment modality.

In a preliminary clinical study, Arora et al. synthesized $^{177}$Lu-labeled tin colloid (mean size: 241±47 nm) and injected into the infected knee joint of a patient [183]. SPECT scan revealed homogenous distribution of the product in the intra-articular space. No leakage of activity was observed outside the knee joint even 7 days after injection, indicating good binding of the radiolabeled agent and its *in vivo* stability. As an extension of this work, the same group of authors evaluated the efficacy of $^{177}$Lu-labeled tin colloid in 29 patients with chronic synovitis caused by various inflammatory knee joint diseases which were refractory to conventional therapy [184]. Out of the 29 patients, 21 were responders and 8 were non-responders at 3 months after radiation synovectomy. No serious adverse effects were observed in any of the patients. The authors concluded that $^{177}$Lu-labeled tin colloid is a useful treatment modality and is beneficial for the patients with shorter duration of disease and with normal or minor radiographic findings. In a recent study, the same group of authors further compared the clinical efficacy of $^{177}$Lu-labeled tin colloid with $^{188}$Re-labeled tin chloride for radiation synovectomy to reduce pain in patients with chronic inflammatory arthritis of knee [185]. The authors administered $^{188}$Re-labeled tin chloride in 27 patients and $^{177}$Lu-labeled tin colloid in 30 patients. Out of 30, 20 patients responded to radiosynovectomy with $^{177}$Lu-labeled tin colloid and 21 patients out of 27 responded to the same with $^{188}$Re-labeled tin colloid. Overall, the authors concluded that $^{177}$Lu-labeled tin colloid is an effective alternative to $^{188}$Re-labeled tin colloid for radiation synovectomy especially in places which do not have access to $^{188}$W/$^{188}$Re generators.

*Radiolabeled nanoparticles*

Over the last decade, a large variety of radiolabeled nanoparticles have been synthesized and assessed for their possible use in cancer

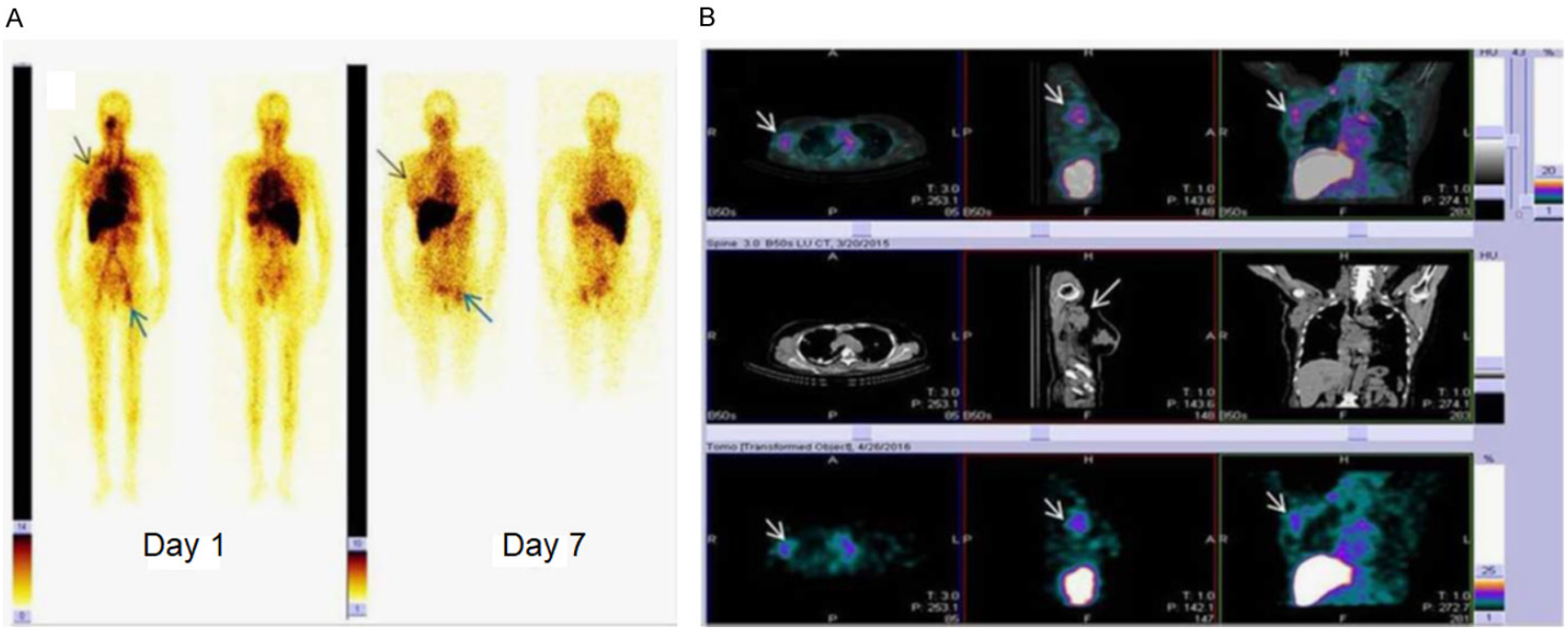


**Figure 13.** A 60-year-old breast cancer patient (HER2 +ve) was administered with $^{177}$Lu-DOTA-trastuzumab therapy. A. WBS at day 1 and day 7 post administration of $^{177}$Lu-DOTA-trastuzumab. Tracer uptake can be observed in primary breast tumor (black arrow head). The bone metastasis in the acetabulum region was visualized at day 1 and day 7 (blue arrow heads). B. SPECT/CT, CT, and SPECT images showing lymph node metastases which could not be localized on WBS (white arrow heads). Adapted from Ref [171].

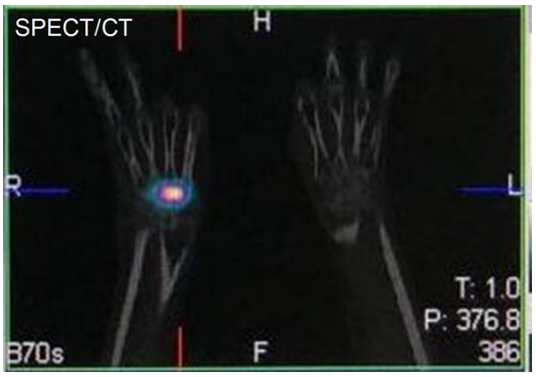


**Figure 14.** A 56-year-old male patient with rheumatoid arthritis of wrist joint. SPECT/CT image 24 h post-administration of 222 MBq of $^{177}$Lu-HA.

imaging and therapy [186-198]. The advantages of using radiolabeled nanoparticles for this purpose are manifold [194]. Firstly, compared to conventional radiotracers, radiolabeled nanoparticles act as signal amplifiers leading to increased contrast indices and enhanced sensitivity. Secondly, nanoparticles can be conjugated with variety of targeting ligands such as peptides, antibodies, aptamers for enhanced uptake and retention by active targeting in addition to enhanced permeability and retention (EPR) effect. Thirdly, nanoparticles offer the scope of multimodality imaging which provides synergistic advantages over any single imaging modality. Fourthly, both diagnostic and therapeutic capabilities can be integrated in the same nanoplatform, thereby giving the benefits of theranostics. Finally, different therapeutic modalities (chemotherapy, radionuclide therapy, etc.) can be incorporated in the same nanoplatforms giving rise to enhanced therapeutic benefits.

For the first time, Arora et al. reported the synthesis of poly(D,L-Lactide-co-Glycolide) (PLGA) nanospheres coated with polyethylene glycol (PEG) [199]. The nanoparticles were spherical in shape with mean particle diameter of ~300 nm. $^{177}$Lu-DOTATATE was encapsulated with >75% efficiency in the synthesized nanoparticles by incubating the nanoparticles with the radiolabeled agent at 37°C, overnight. The authors performed *in vivo* SPECT imaging and biodistribution studies in normal rats after intravenous administration of the radiolabeled nanoparticles and observed reduced renal retention of $^{177}$Lu-DOTATATE. These results suggest the potential of this strategy in achieving reduction in nephrotoxicity and unnecessary radiation dose to the normal tissue, which might have implications in targeted therapy of neuroendocrine tumors. Subsequently, in another study, the same group of authors evaluated the *in vitro* toxicity of the radiolabeled nanoparticles in U87MG (human glioblastoma) cell line [200]. The highest cytotoxicity that could be achieved on radioresistant U87MG cells was 35.8%. *In vivo* SPECT imaging and biodistribution studies in tumor bearing Wistar rats showed the highest tumor uptake of ~4.5% ID/g at 24 h post-injection (p.i.). The main limitations of these studies are the very slow method of radiolabeling and the lack of data to prove the therapeutic potential of the radiolabeled nanoparticles.

Recently, attempts have been made towards synthesis of intrinsically radiolabeled nanoparticles which represents a new paradigm in nanomedicine research [201-210]. The intrinsically radiolabeled nanoparticles offer several advantages over the conventional chelator-based radiolabeling techniques: this approach offers highly efficient, radiochemically more stable, faster and robust radiolabeling possibilities without changing the innate pharmacokinetics of the nanoparticles. This strategy is especially advantageous for low specific activity radioisotopes such as $^{177}$Lu produced by direct neutron activation route using natural targets for development of effective therapeutic agents. In this direction, our group has reported the synthesis of intrinsically radiolabeled [$^{177}$Lu]$Lu_2O_3$ nanoparticles entrapped in human serum albumin scaffold, as schematically illustrated in **Figure 15** [211]. The particle size of the nanoparticles was in the range of 2-6 nm. *In vitro* cell binding and toxicity studies in murine melanoma (B16F10) cells demonstrated the suitability of the radiolabeled nanoparticles as a therapeutic agent. *Ex vivo* biodistribution studies in melanoma tumor bearing mice demonstrated fast and high accumulation of the radiolabeled nanoparticles in the tumor (11.7±2.1% ID/g at 4 h p.i.) with significant retention up to 7 days. The therapeutic efficacy of the intrinsically radiolabeled nanoparticles was demonstrated by tumor regression studies performed over a period of 21 days (**Figure 16**). The promising results obtained in this study demonstrate the poten-

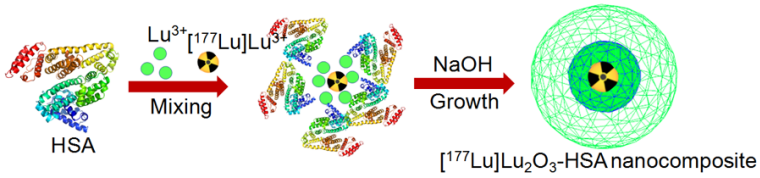


**Figure 15.** Schematic illustration of the synthesis of intrinsically radiolabeled [$^{177}$Lu]$Lu_2O_3$-HSA nanocomposite. Adapted from Ref [211].

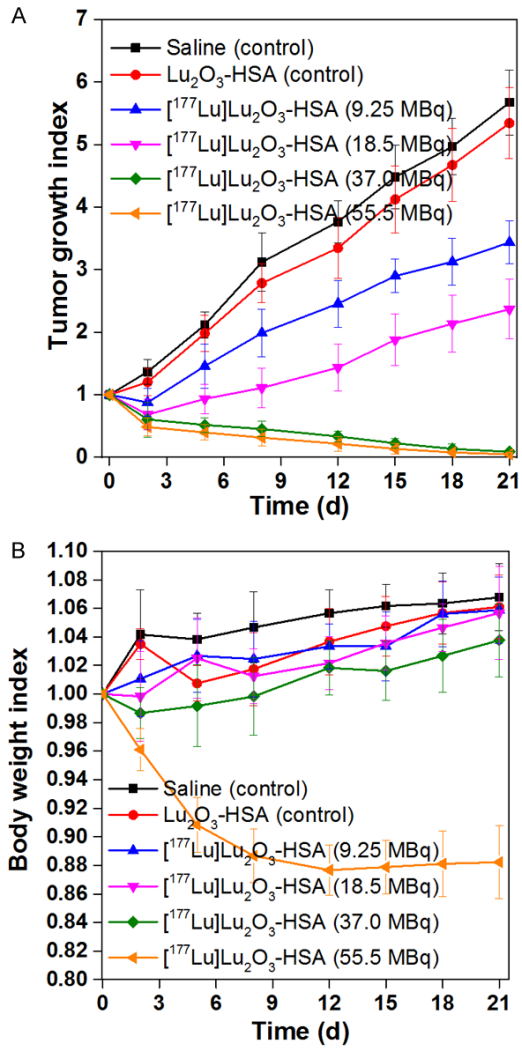


**Figure 16.** Tumor regression studies with [$^{177}$Lu]$Lu_2O_3$-HSA nanocomposite. (A) Tumor growth index and (B) body weight index curves of C57BL/6 mice bearing melanoma tumor after intravenous injection of saline (control), $Lu_2O_3$-HSA (control), 9.25 MBq of [$^{177}$Lu]$Lu_2O_3$-HSA nanocomposite, 18.5 MBq [$^{177}$Lu]$Lu_2O_3$-HSA nanocomposite, 37 MBq [$^{177}$Lu]$Lu_2O_3$-HSA nanocomposite and 55.5 MBq [$^{177}$Lu]$Lu_2O_3$-HSA nanocomposite. Adapted from Ref [211].

tial of this class of radiolabeled nanoparticles for potential clinical translation.

## Conclusions

In this treatise, the multifaceted aspects of $^{177}$Lu-radiopharmacy were discussed emphasizing on the utility of $^{177}$Lu produced via direct neutron activation route over the last decade in clinical context. Surely, $^{177}$Lu has emerged as the most widely used therapeutic radioisotope after $^{131}$I and the clinical efficacies of several $^{177}$Lu-based radiopharmaceuticals have amply been demonstrated. The favorable nuclear decay characteristics and the widespread and affordable availability of the radioisotope are the main reasons behind its widespread clinical use. The relatively long half-life of $^{177}$Lu provides distinct logistic advantages especially in countries with limited reactor facilities for radioisotope production. The feasibility of large-scale production with adequate specific activity in medium flux research reactors via facile direct neutron activation route is another desirable feature for widespread utilization of this radioisotope. According to the IAEA research reactor database [31], there are >250 operational nuclear reactors worldwide, out of which 50 reactors have thermal neutron flux over 1 × $10^{14}$ n.cm$^{-2}$.s$^{-1}$ which is acceptable for production of $^{177}$Lu by the direct route for preparation of target specific radiopharmaceuticals. These reactors have good geographical distribution and hence their utilization would ensure cost-effective and widespread utilization of $^{177}$Lu for clinical use.

Though, some groups especially in the developed countries have preference for NCA $^{177}$Lu in view of its higher specific activity, the production of the radioisotope by the indirect route is still a costly proposition and requires access to high flux research reactors, very few of which are presently available in the world. In the indirect route, only a very small fraction of the enriched $^{176}$Yb target is transformed into $^{177}$Lu due to the low cross section of $^{176}$Yb. The $^{177}$Lu recovery from the target requires the employment of effective Lu/Yb separation methods, whose characteristics are not only crucial for the practicality of the indirect production route but also increases the overall cost. In this review, the practical and unclear issues regarding production of $^{177}$Lu by both the routes in a nuclear reactor were discussed

to provide the readers an in-depth holistic overview regarding the production aspects.

The chemistry of $^{177}$Lu in the form of $Lu^{3+}$ allows for facile radiolabeling either directly with different biomolecules such as EDTMP and DOTMP or through the use of BFCs. Among the various BFCs studied, DOTA is undoubtedly the 'gold standard' in preparation of $^{177}$Lu-based radiopharmaceuticals. Complexes of $^{177}$Lu with DOTA and its derivatives are formed with high radiochemical yield and they exhibit excellent *in vitro* and *in vivo* stability. However, the kinetics of the complexation process with macrocyclic DOTA chelator is slow and requires heating at ~90°C for achieving near quantitative yield. This is in fact undesirable for radiolabeling temperature sensitive biomolecules such as monoclonal antibodies. From this perspective, the new AAZTA chelator which manifests rapid room temperature radiolabeling with high stability is a valuable proposition and would especially be advantageous towards $^{177}$Lu-based radioimmunotherapy. The use of AAZTA chelator would also simplify the radiopharmacy practices for other $^{177}$Lu-based theranostic agents.

Till recently, $^{177}$Lu-DOTATATE held the distinction of being the most widely used $^{177}$Lu-based radiopharmaceutical, which has now been overtaken by $^{177}$Lu-PSMA-617 because of the much larger number of prostate cancer cases compared to neuroendocrine tumors. Together, $^{177}$Lu-PSMA-617 and $^{177}$Lu-DOTATATE encompass for use of >90% of the $^{177}$Lu produced worldwide. It has been amply demonstrated from the large number of clinical studies summarized in this review that even while using medium specific activity $^{177}$Lu produced by the direct neutron activation route, $^{177}$Lu based radiopharmaceuticals can be prepared with adequate radiochemical purity and specific activity for effective and efficient targeted cancer therapy. The concept of intrinsically radiolabeled nanoparticles is an emerging concept in personalized cancer therapy which would aid toward development of agents which show enhanced tumor targeting even while using low specific activity $^{177}$Lu produced by inexpensive natural Lu target. However, for clinical translation of this emerging therapeutic modality, synthesis of biocompatible and biodegradable nanoplatforms which demonstrate renal clearable properties to minimize toxicity concerns is desirable [212-216]. Also, there is an ever-increasing possibility of identifying new molecular targeting vectors such as new peptides, monoclonal antibodies and their engineered fragments, nanobodies, aptamers, etc. for synthesis of new generation of $^{177}$Lu based radiopharmaceuticals for personalized cancer treatment. The present advances are just the tip of the iceberg and more exciting avenues are yet to open up. To explore the 'gold mine' of $^{177}$Lu-radiopharmacy to its fullest potential, increased interdisciplinary collaboration and knowledge exchange among various stakeholders in this field, which include, funding agencies, regulatory authorities, clinicians, and scientists should be encouraged for development and clinical deployment of newer $^{177}$Lu-based agents for the benefit of the millions of cancer patients worldwide.

## Disclosure of conflict of interest

None.

**Address correspondence to:** Dr. Rubel Chakravarty, Radiopharmaceuticals Division, Bhabha Atomic Research Centre, Trombay, Mumbai 400085, India. Tel: +91-22-25590624; Fax: +91-22-255-05151; E-mail: rubelc@barc.gov.in; rubelchakravarty@gmail.com

## References

[1] Turner JH. Recent advances in theranostics and challenges for the future. Br J Radiol 2018; 91: 20170893.
[2] Choudhury P and Gupta M. Personalized & precision medicine in cancer: a theranostic approach. Curr Radiopharm 2017; 10: 166-170.
[3] Farolfi A, Lima GM, Oyen W and Fanti S. Molecular imaging and theranostics-a multidisciplinary approach. Semin Nucl Med 2019; 49: 247-254.
[4] Filippi L, Chiaravalloti A, Schillaci O, Cianni R and Bagni O. Theranostic approaches in nuclear medicine: current status and future prospects. Expert Rev Med Devices 2020; 17: 331-343.
[5] Jeelani S, Reddy RC, Maheswaran T, Asokan GS, Dany A and Anand B. Theranostics: a treasured tailor for tomorrow. J Pharm Bioallied Sci 2014; 6: S6-8.
[6] Boros E and Packard AB. Radioactive transition metals for imaging and therapy. Chem Rev 2019; 119: 870-901.
[7] Brandt M, Cardinale J, Aulsebrook ML, Gasser G and Mindt TL. An overview of PET radiochemistry, part 2: radiometals. J Nucl Med 2018; 59: 1500-1506.
[8] Kostelnik TI and Orvig C. Radioactive main group and rare Earth metals for imaging and therapy. Chem Rev 2019; 119: 902-956.

[9] Mikolajczak R, van der Meulen NP and Lapi SE. Radiometals for imaging and theranostics, current production, and future perspectives. J Labelled Comp Radiopharm 2019; 62: 615-634.
[10] Notni J and Wester HJ. Re-thinking the role of radiometal isotopes: towards a future concept for theranostic radiopharmaceuticals. J Labelled Comp Radiopharm 2018; 61: 141-153.
[11] Dash A, Pillai MR and Knapp FF Jr. Production of $^{177}$Lu for targeted radionuclide therapy: available options. Nucl Med Mol Imaging 2015; 49: 85-107.
[12] Banerjee S, Pillai MR and Knapp FF. Lutetium-177 therapeutic radiopharmaceuticals: linking chemistry, radiochemistry, and practical applications. Chem Rev 2015; 115: 2934-2974.
[13] Hermanne A, Takacs S, Goldberg MB, Lavie E, Shubin YN and Kovalev S. Deuteron-induced reactions on Yb: measured cross sections and rationale for production pathways of carrier-free, medically relevant radionuclides. Nucl Instrum Methods Phys Res B 2006; 247: 223-231.
[14] Manenti S, Groppi F, Gandini A, Gini L, Abbas K, Holzwarth U, Simonelli F and Bonardi M. Excitation function for deuteron induced nuclear reactions on natural ytterbium for production of high specific activity $^{177g}$Lu in no-carrier-added form for metabolic radiotherapy. Appl Radiat Isot 2011; 69: 37-45.
[15] Khandaker MU, Haba H and Kassim HA. Production of $^{177}$Lu, a potential radionuclide for diagnostic and therapeutic applications. AIP Conf Proc 2015; 1657: 120003.
[16] Manenti S, Bonardi ML, Gini L and Groppi F. Physical optimization of production by deuteron irradiation of high specific activity $^{177g}$Lu suitable for radioimmunotherapy. Nucl Med Biol 2014; 41: 407-409.
[17] Kambali I. Production of Lu-177 radionuclide using deuteron beams: comparison between (d,n) and (d,p) nuclear reactions. J Phys Conf Ser 2018; 1120: 012011.
[18] Medvedev DG, Mausner LF, Greene GA and Hanson AL. Activation of natural Hf and Ta in relation to the production of $^{177}$Lu. Appl Radiat Isot 2008; 66: 1300-1306.
[19] Kuznetsov RA, Bobrovskaya KS, Svetukhin VV, Fomin AN and Zhukov AV. Production of lutetium-177: process aspects. Radiochemistry 2019; 61: 381-395.
[20] Dash A, Chakravarty R, Knapp FF Jr and Pillai AM. Indirect production of no carrier added (NCA) $^{177}$Lu from irradiation of enriched $^{176}$Yb: options for ytterbium/lutetium separation. Curr Radiopharm 2015; 8: 107-118.
[21] Vosoughi S, Salek N, Arani SS, Samani AB and Maragheh MG. Investigation of radiolabeling efficacy by enhancement of the chemical form of no carrier added $^{177}$Lu isolated by electro amalgamation process. Curr Radiopharm 2021; [Epub ahead of print].
[22] Chakravarty R, Das T, Dash A and Venkatesh M. An electro-amalgamation approach to isolate no-carrier-added $^{177}$Lu from neutron irradiated Yb for biomedical applications. Nucl Med Biol 2010; 37: 811-820.
[23] Mikolajczak R, Parus JL, Pawlak D, Zakrzewska E, Michalak W and Sasinowska I. Reactor produced $^{177}$Lu of specific activity and purity suitable for medical applications. J Radioanal Nucl Chem 2003; 257: 53-57.
[24] Van So L, Morcos N, Zaw M, Pellegrini P and Greguric I. Alternative chromatographic processes for no-carrier added $^{177}$Lu radioisotope separation. J Radioanal Nucl Chem 2008; 277: 663.
[25] Horwitz EP, McAlister DR, Bond AH, Barrans RE and Williamson JM. A process for the separation of $^{177}$Lu from neutron irradiated $^{176}$Yb targets. Appl Radiat Isot 2005; 63: 23-36.
[26] Hashimoto K, Matsuoka H and Uchida S. Production of no-carrier-added $^{177}$Lu via the $^{176}$Yb(n,γ)$^{177}$Yb→$^{177}$Lu process. J Radioanal Nucl Chem 2003; 255: 575-579.
[27] Lebedev NA, Novgorodov AF, Misiak R, Brockmann J and Rösch F. Radiochemical separation of no-carrier-added $^{177}$Lu as produced via the $^{176}$Yb(n,gamma)$^{177}$Yb→$^{177}$Lu process. Appl Radiat Isot 2000; 53: 421-425.
[28] Lahiri S, Nayak D, Nandy M and Das NR. Separation of carrier free lutetium produced in proton activated ytterbium with HDEHP. Appl Radiat Isot 1998; 49: 911-913.
[29] Dvorakova Z. Production and chemical processing of 177Lu for nuclear medicine at the Munich research reactor FRM-II. Ph.D. Thesis (Available online at: https://mediatum.ub.tum.de/doc/625564/document.pdf 2007; Accessed on September 1, 2021).
[30] Chakraborty S, Vimalnath KV, Lohar SP, Shetty P and Dash A. On the practical aspects of large-scale production of $^{177}$Lu for peptide receptor radionuclide therapy using direct neutron activation of $^{176}$Lu in a medium flux research reactor: the Indian experience. J Radioanal Nucl Chem 2014; 302: 233-243.
[31] IAEA Research Reactor Database (https://nucleus.iaea.org/RRDB/RR/ReactorSearch.aspx) Accessed on September 1, 2021.
[32] Liu S. Bifunctional coupling agents for radiolabeling of biomolecules and target-specific delivery of metallic radionuclides. Adv Drug Deliv Rev 2008; 60: 1347-1370.
[33] Bailey GA, Price EW, Zeglis BM, Ferreira CL, Boros E, Lacasse MJ, Patrick BO, Lewis JS, Adam MJ and Orvig C. $H_2$azapa: a versatile acyclic multifunctional chelator for $^{67}$Ga, $^{64}$Cu, $^{111}$In,

and $^{177}$Lu. Inorg Chem 2012; 51: 12575-12589.
[34] Brechbiel MW. Bifunctional chelates for metal nuclides. Q J Nucl Med Mol Imaging 2008; 52: 166-173.
[35] Parus JL, Pawlak D, Mikolajczak R and Duatti A. Chemistry and bifunctional chelating agents for binding $^{177}$Lu. Curr Radiopharm 2015; 8: 86-94.
[36] Boros E and Holland JP. Chemical aspects of metal ion chelation in the synthesis and application antibody-based radiotracers. J Labelled Comp Radiopharm 2018; 61: 652-671.
[37] Deng H, Wang H and Li Z. Matching chelators to radiometals for positron emission tomography imaging-guided targeted drug delivery. Curr Drug Targets 2015; 16: 610-624.
[38] Park JA and Kim JY. Recent advances in radiopharmaceutical application of matched-pair radiometals. Curr Top Med Chem 2013; 13: 458-469.
[39] Price EW and Orvig C. Matching chelators to radiometals for radiopharmaceuticals. Chem Soc Rev 2014; 43: 260-290.
[40] Price EW, Zeglis BM, Cawthray JF, Lewis JS, Adam MJ and Orvig C. What a difference a carbon makes: $H_4$octapa vs $H_4C_3$octapa, ligands for In-111 and Lu-177 radiochemistry. Inorg Chem 2014; 53: 10412-10431.
[41] Ramogida CF and Orvig C. Tumour targeting with radiometals for diagnosis and therapy. Chem Commun (Camb) 2013; 49: 4720-4739.
[42] Askari E, Harsini S, Vahidfar N, Divband G and Sadeghi R. $^{177}$Lu-EDTMP for metastatic bone pain palliation: a systematic review and meta-analysis. Cancer Biother Radiopharm 2021; 36: 383-390.
[43] Zakaly HMH, Mostafa MYA, Deryabina D and Zhukovsky M. Comparative studies on the potential use of $^{177}$Lu-based radiopharmaceuticals for the palliative therapy of bone metastases. Int J Radiat Biol 2020; 96: 779-789.
[44] Chakraborty S, Vimalnath KV, Rajeswari A, Chakravarty R, Sarma HD, Radhakrishnan E, Kamaleshwaran K, Shinto AS and Dash A. A "mix-and-use" approach for formulation of human clinical doses of $^{177}$Lu-DOTMP at hospital radiopharmacy for management of pain arising from skeletal metastases. J Labelled Comp Radiopharm 2017; 60: 410-419.
[45] Das T, Shinto A, Karuppuswamy Kamaleshwaran K and Banerjee S. Theranostic treatment of metastatic bone pain with $^{177}$Lu-DOTMP. Clin Nucl Med 2016; 41: 966-967.
[46] Kumar C, Sharma R, Das T, Korde A, Sarma H, Banerjee S and Dash A. $^{177}$Lu-DOTMP induces G2/M cell cycle arrest and apoptosis in MG63 cell line. J Labelled Comp Radiopharm 2018; 61: 837-846.
[47] De León-Rodríguez LM and Kovacs Z. The synthesis and chelation chemistry of DOTA-peptide conjugates. Bioconjug Chem 2008; 19: 391-402.
[48] Parry JJ, Kelly TS, Andrews R and Rogers BE. In vitro and in vivo evaluation of $^{64}$Cu-labeled DOTA-linker-bombesin(7-14) analogues containing different amino acid linker moieties. Bioconjug Chem 2007; 18: 1110-1117.
[49] Hernandez R, Czerwinski A, Chakravarty R, Graves SA, Yang Y, England CG, Nickles RJ, Valenzuela F and Cai W. Evaluation of two novel $^{64}$Cu-labeled RGD peptide radiotracers for enhanced PET imaging of tumor integrin $\alpha v\beta_3$. Eur J Nucl Med Mol Imaging 2015; 42: 1859-1868.
[50] Guzik P, Siwowska K, Fang HY, Cohrs S, Bernhardt P, Schibli R and Müller C. Promising potential of [$^{177}$Lu]Lu-DOTA-folate to enhance tumor response to immunotherapy-a preclinical study using a syngeneic breast cancer model. Eur J Nucl Med Mol Imaging 2021; 48: 984-994.
[51] Hänscheid H, Hartrampf PE, Schirbel A, Buck AK and Lapa C. Intraindividual comparison of [$^{177}$Lu]Lu-DOTA-EB-TATE and [$^{177}$Lu]Lu-DOTA-TOC. Eur J Nucl Med Mol Imaging 2021; 48: 2566-2572.
[52] Miranda ACC, Durante ACR, Fuscaldi LL, Barbezan AB, de Lima CR, Perini E and de Araújo EB. Anti-HER2 monoclonal antibody based-radioimmunoconjugates: assessment of the chelating agent influence. Bioorg Med Chem 2021; 33: 115996.
[53] Akbar MU, Bokhari TH, Ahmad MR, Zia KM, Roohi S, Ayub N and Sohaib M. Radiosynthesis, radiochemical, and biological characterization of $^{177}$Lu-labeled diethylenetriamine penta-acetic acid. J Cell Biochem 2019; 120: 14510-14517.
[54] Ehlerding EB, Lacognata S, Jiang D, Ferreira CA, Goel S, Hernandez R, Jeffery JJ, Theuer CP and Cai W. Targeting angiogenesis for radioimmunotherapy with a $^{177}$Lu-labeled antibody. Eur J Nucl Med Mol Imaging 2018; 45: 123-131.
[55] Shi J, Liu Z, Jia B, Yu Z, Zhao H and Wang F. Potential therapeutic radiotracers: preparation, biodistribution and metabolic characteristics of $^{177}$Lu-labeled cyclic RGDfK dimer. Amino Acids 2010; 39: 111-120.
[56] Tsai WK, Zettlitz KA, Dahlbom M, Reiter RE and Wu AM. Evaluation of [$^{131}$I]I- and [$^{177}$Lu]Lu-DTPA-A11 minibody for radioimmunotherapy in a preclinical model of PSCA-expressing prostate cancer. Mol Imaging Biol 2020; 22: 1380-1391.
[57] Zhou L, Chen L, Yang L, Cai L, Liu L, Zhao Y, Feng Y, Liu N, Zhao Y, Xia Y, Wei H and Chen Y. Preliminary studies of $^{177}$Lu-diethylenetriamine

penta-acetic acid-deoxyglucose in hepatic tumor-bearing mice. Cancer Biother Radiopharm 2020; 35: 33-40.
[58] Greifenstein L, Grus T, Nagel J, Sinnes JP and Rösch F. Synthesis and labeling of a squaric acid containing PSMA-inhibitor coupled to AAZTA(5) for versatile labeling with $^{44}$Sc, $^{64}$Cu, $^{68}$Ga and $^{177}$Lu. Appl Radiat Isot 2020; 156: 108867.
[59] Pfister J, Summer D, Rangger C, Petrik M, von Guggenberg E, Minazzi P, Giovenzana GB, Aloj L and Decristoforo C. Influence of a novel, versatile bifunctional chelator on theranostic properties of a minigastrin analogue. EJNMMI Res 2015; 5: 74.
[60] Sinnes JP, Bauder-Wüst U, Schäfer M, Moon ES, Kopka K and Rösch F. $^{68}$Ga, $^{44}$Sc and $^{177}$Lu-labeled AAZTA(5)-PSMA-617: synthesis, radiolabeling, stability and cell binding compared to DOTA-PSMA-617 analogues. EJNMMI Radiopharm Chem 2020; 5: 28.
[61] Sinnes JP, Nagel J and Rösch F. AAZTA(5)/AAZTA(5)-TOC: synthesis and radiochemical evaluation with $^{68}$Ga, $^{44}$Sc and $^{177}$Lu. EJNMMI Radiopharm Chem 2019; 4: 18.
[62] Ambrosini V, Kunikowska J, Baudin E, Bodei L, Bouvier C, Capdevila J, Cremonesi M, de Herder WW, Dromain C, Falconi M, Fani M, Fanti S, Hicks RJ, Kabasakal L, Kaltsas G, Lewington V, Minozzi S, Cinquini M, Öberg K, Oyen WJG, O'Toole D, Pavel M, Ruszniewski P, Scarpa A, Strosberg J, Sundin A, Taïeb D, Virgolini I, Wild D, Herrmann K and Yao J. Consensus on molecular imaging and theranostics in neuroendocrine neoplasms. Eur J Cancer 2021; 146: 56-73.
[63] Amini A, Dehdar F, Jafari E, Gholamrezanezhad A and Assadi M. Somatostatin receptor scintigraphy in a patient with myocarditis. Mol Imaging Radionucl Ther 2021; 30: 50-53.
[64] Xu C and Zhang H. Somatostatin receptor based imaging and radionuclide therapy. Biomed Res Int 2015; 2015: 917968.
[65] Kwekkeboom DJ, de Herder WW and Krenning EP. Somatostatin receptor-targeted radionuclide therapy in patients with gastroenteropancreatic neuroendocrine tumors. Endocrinol Metab Clin North Am 2011; 40: 173-185, ix.
[66] Patel YC, Greenwood MT, Panetta R, Demchyshyn L, Niznik H and Srikant CB. The somatostatin receptor family. Life Sci 1995; 57: 1249-1265.
[67] Bruns C, Weckbecker G, Raulf F, Lübbert H and Hoyer D. Characterization of somatostatin receptor subtypes. Ciba Found Symp 1995; 190: 89-101; discussion 101-10.
[68] Schonbrunn A, Gu YZ, Brown PJ and Loose-Mitchell D. Function and regulation of somatostatin receptor subtypes. Ciba Found Symp 1995; 190: 204-217.
[69] Brabander T, Nonnekens J and Hofland J. The next generation of peptide receptor radionuclide therapy. Endocr Relat Cancer 2019; 26: C7-C11.
[70] Cordova C and Kurz SC. Advances in molecular classification and therapeutic opportunities in meningiomas. Curr Oncol Rep 2020; 22: 84.
[71] Das S, Al-Toubah T, El-Haddad G and Strosberg J. $^{177}$Lu-DOTATATE for the treatment of gastroenteropancreatic neuroendocrine tumors. Expert Rev Gastroenterol Hepatol 2019; 13: 1023-1031.
[72] Kendi AT, Halfdanarson TR, Packard A, Dundar A and Subramaniam RM. Therapy With (177) Lu-DOTATATE: clinical implementation and impact on care of patients with neuroendocrine tumors. AJR Am J Roentgenol 2019; 213: 309-317.
[73] Mittra ES. Neuroendocrine tumor therapy: $^{177}$Lu-DOTATATE. AJR Am J Roentgenol 2018; 211: 278-285.
[74] Ramage J, Naraev BG and Halfdanarson TR. Peptide receptor radionuclide therapy for patients with advanced pancreatic neuroendocrine tumors. Semin Oncol 2018; 45: 236-248.
[75] Satapathy S and Mittal BR. $^{177}$Lu-DOTATATE peptide receptor radionuclide therapy versus everolimus in advanced pancreatic neuroendocrine tumors: a systematic review and meta-analysis. Nucl Med Commun 2019; 40: 1195-1203.
[76] Satapathy S, Mittal BR and Bhansali A. 'Peptide receptor radionuclide therapy in the management of advanced pheochromocytoma and paraganglioma: a systematic review and meta-analysis'. Clin Endocrinol (Oxf) 2019; 91: 718-727.
[77] Wang LF, Lin L, Wang MJ and Li Y. The therapeutic efficacy of $^{177}$Lu-DOTATATE/DOTATOC in advanced neuroendocrine tumors: a meta-analysis. Medicine (Baltimore) 2020; 99: e19304.
[78] Zhang J, Song Q, Cai L, Xie Y and Chen Y. The efficacy of $^{177}$Lu-DOTATATE peptide receptor radionuclide therapy (PRRT) in patients with metastatic neuroendocrine tumours: a systematic review and meta-analysis. J Cancer Res Clin Oncol 2020; 146: 1533-1543.
[79] Basu S, Chakraborty S, Parghane RV, Kamaldeep, Ranade R, Thapa P, Asopa RV, Sonawane G, Nabar S, Shimpi H, Chandak A, Vimalnath KV, Ostwal V, Ramaswamy A, Bhandare M, Chaudhari V, Shrikhande SV, Sirohi B, Dash A and Banerjee S. One decade of 'Bench-to-Bedside' peptide receptor radionuclide therapy with indigenous [$^{177}$Lu]Lu-DOTATATE obtained through 'Direct' neutron activation route: lessons learnt including practice evolu-

tion in an Indian setting. Am J Nucl Med Mol Imaging 2020; 10: 178-211.
[80] Das T, Chakraborty S, Banerjee S and Venkatesh M. On the preparation of a therapeutic dose of $^{177}$Lu-labeled DOTA-TATE using indigenously produced $^{177}$Lu in medium flux reactor. Appl Radiat Isot 2007; 65: 301-308.
[81] Das T, Chakraborty S, Kallur KG, Venkatesh M and Banerjee S. Preparation of patient doses of $^{177}$Lu-DOTA-TATE using indigenously produced $^{177}$Lu: the Indian experience. Cancer Biother Radiopharm 2011; 26: 395-400.
[82] Mathur A, Prashant V, Sakhare N, Chakraborty S, Vimalnath KV, Mohan RK, Arjun C, Karkhanis B, Seshan R, Basu S, Korde A, Banerjee S, Dash A and Sachdev SS. Bulk scale formulation of therapeutic doses of clinical grade ready-to-use $^{177}$Lu-DOTA-TATE: the intricate radiochemistry aspects. Cancer Biother Radiopharm 2017; 32: 266-273.
[83] Dash A, Chakraborty S, Pillai MR and Knapp FF Jr. Peptide receptor radionuclide therapy: an overview. Cancer Biother Radiopharm 2015; 30: 47-71.
[84] Gupta SK, Singla S and Bal C. Renal and hematological toxicity in patients of neuroendocrine tumors after peptide receptor radionuclide therapy with $^{177}$Lu-DOTATATE. Cancer Biother Radiopharm 2012; 27: 593-599.
[85] Gupta SK, Singla S, Thakral P and Bal CS. Dosimetric analyses of kidneys, liver, spleen, pituitary gland, and neuroendocrine tumors of patients treated with $^{177}$Lu-DOTATATE. Clin Nucl Med 2013; 38: 188-194.
[86] Jois B, Asopa R and Basu S. Somatostatin receptor imaging in non-$^{131}$I-avid metastatic differentiated thyroid carcinoma for determining the feasibility of peptide receptor radionuclide therapy with $^{177}$Lu-DOTATATE: low fraction of patients suitable for peptide receptor radionuclide therapy and evidence of chromogranin A level-positive neuroendocrine differentiation. Clin Nucl Med 2014; 39: 505-510.
[87] Basu S and Ranade R. Favorable response of metastatic merkel cell carcinoma to targeted $^{177}$Lu-DOTATATE therapy: will PRRT evolve to become an important approach in receptor-positive cases? J Nucl Med Technol 2016; 44: 85-87.
[88] Danthala M, Kallur KG, Prashant GR, Rajkumar K and Raghavendra Rao M. $^{177}$Lu-DOTATATE therapy in patients with neuroendocrine tumours: 5 years' experience from a tertiary cancer care centre in India. Eur J Nucl Med Mol Imaging 2014; 41: 1319-1326.
[89] Ballal S, Yadav MP, Damle NA, Sahoo RK and Bal C. Concomitant $^{177}$Lu-DOTATATE and capecitabine therapy in patients with advanced neuroendocrine tumors: a long-term-outcome, toxicity, survival, and quality-of-life study. Clin Nucl Med 2017; 42: e457-e466.
[90] Yadav MP, Ballal S and Bal C. Concomitant $^{177}$Lu-DOTATATE and capecitabine therapy in malignant paragangliomas. EJNMMI Res 2019; 9: 13.
[91] Basu S, Parghane RV and Banerjee S. Availability of both [$^{177}$Lu]Lu-DOTA-TATE and [$^{90}$Y]Y-DOTATATE as PRRT agents for neuroendocrine tumors: can we evolve a rational sequential duo-PRRT protocol for large volume resistant tumors? Eur J Nucl Med Mol Imaging 2020; 47: 756-758.
[92] Parghane RV, Naik C, Talole S, Desmukh A, Chaukar D, Banerjee S and Basu S. Clinical utility of $^{177}$Lu-DOTATATE PRRT in somatostatin receptor-positive metastatic medullary carcinoma of thyroid patients with assessment of efficacy, survival analysis, prognostic variables, and toxicity. Head Neck 2020; 42: 401-416.
[93] Parghane RV, Talole S and Basu S. Prevalence of hitherto unknown brain meningioma detected on $^{68}$Ga-DOTATATE positron-emission tomography/computed tomography in patients with metastatic neuroendocrine tumor and exploring potential of $^{177}$Lu-DOTATATE peptide receptor radionuclide therapy as single-shot treatment approach targeting both tumors. World J Nucl Med 2019; 18: 160-170.
[94] Parghane RV, Mitra A, Upadhye T, Rakshit S, Banerjee S and Basu S. Sequential duo-peptide receptor radionuclide therapy with indigenous $^{90}$Y-DOTATATE and $^{177}$Lu-DOTATATE in large-volume neuroendocrine tumors: post-therapy bremsstrahlung and pet/ct imaging following $^{90}$Y-DOTATATE treatment. Clin Nucl Med 2020; 45: 714-715.
[95] Parghane RV, Ostwal V, Ramaswamy A, Bhandare M, Chaudhari V, Talole S, Shrikhande SV and Basu S. Long-term outcome of "Sandwich" chemo-PRRT: a novel treatment strategy for metastatic neuroendocrine tumors with both FDG- and SSTR-avid aggressive disease. Eur J Nucl Med Mol Imaging 2021; 48: 913-923.
[96] Sitani K, Parghane RV, Talole S and Basu S. Long-term outcome of indigenous $^{177}$Lu-DOTATATE PRRT in patients with metastatic advanced neuroendocrine tumours: a single institutional observation in a large tertiary care setting. Br J Radiol 2021; 94: 20201041.
[97] Parghane RV, Talole S and Basu S. $^{131}$I-MIBG negative progressive symptomatic metastatic paraganglioma: response and outcome with $^{177}$Lu-DOTATATE peptide receptor radionuclide therapy. Ann Nucl Med 2021; 35: 92-101.
[98] Jaiswal SK, Sarathi V, Memon SS, Garg R, Malhotra G, Verma P, Shah R, Sehemby MK, Patil VA, Jadhav S, Lila AR, Shah NS and Bandgar

TR. $^{177}$Lu-DOTATATE therapy in metastatic/inoperable pheochromocytoma-paraganglioma. Endocr Connect 2020; 9: 864-873.
[99] Adnan A, Kudachi S, Ramesh S, Prabhash K and Basu S. Metastatic or locally advanced mediastinal neuroendocrine tumours: outcome with $^{177}$Lu-DOTATATE-based peptide receptor radionuclide therapy and assessment of prognostic factors. Nucl Med Commun 2019; 40: 947-957.
[100] Adnan A and Basu S. Combined $^{177}$Lu-DOTATATE peptide receptor radionuclide therapy and platinum-based chemotherapy in recurrent, metastatic sinonasal neuroendocrine carcinoma: a promising therapeutic option. J Nucl Med Technol 2020; 48: 292-294.
[101] Kalshetty A, Ramaswamy A, Ostwal V and Basu S. Resistant functioning and/or progressive symptomatic metastatic gastroenteropancreatic neuroendocrine tumors: efficacy of $^{177}$Lu-DOTATATE peptide receptor radionuclide therapy in this setting. Nucl Med Commun 2018; 39: 1143-1149.
[102] Ramesh S, Kudachi S and Basu S. Peptide receptor radionuclide therapy with $^{177}$Lu-DOTATATE in carcinoid heart disease: a contraindication or a promising treatment approach bettering chances for corrective surgery? J Nucl Med Technol 2018; 46: 292-294.
[103] Litwin MS and Tan HJ. The diagnosis and treatment of prostate cancer: a review. JAMA 2017; 317: 2532-2542.
[104] Sumanasuriya S and De Bono J. Treatment of advanced prostate cancer-a review of current therapies and future promise. Cold Spring Harb Perspect Med 2018; 8: a030635.
[105] Pillai MRA, Nanabala R, Joy A, Sasikumar A and Russ Knapp FF. Radiolabeled enzyme inhibitors and binding agents targeting PSMA: effective theranostic tools for imaging and therapy of prostate cancer. Nucl Med Biol 2016; 43: 692-720.
[106] Chakravarty R, Siamof CM, Dash A and Cai W. Targeted α-therapy of prostate cancer using radiolabeled PSMA inhibitors: a game changer in nuclear medicine. Am J Nucl Med Mol Imaging 2018; 8: 247-267.
[107] Bögemann M, Herrmann K, Radtke JP and Rahbar K. PSMA radioligand therapy in patients with advanced prostate cancer. Urologe A 2020; 59: 680-686.
[108] Gupta M, Karthikeyan G, Choudhury PS, Babu Koyyala VP, Sharma M, Jain P, Talwar V, Singh A and Rawal S. A walk with Lu-177 PSMA: how close we have reached from bench to bedside? Cancer Invest 2020; 38: 486-492.
[109] Iravani A, Violet J, Azad A and Hofman MS. Lutetium-177 prostate-specific membrane antigen (PSMA) theranostics: practical nuances and intricacies. Prostate Cancer Prostatic Dis 2020; 23: 38-52.
[110] Satapathy S, Mittal BR and Sood A. Visceral metastases as predictors of response and survival outcomes in patients of castration-resistant prostate cancer treated with 177Lu-labeled prostate-specific membrane antigen radioligand therapy: a systematic review and meta-analysis. Clin Nucl Med 2020; 45: 935-942.
[111] Sun M, Niaz MO, Nelson A, Skafida M and Niaz MJ. Review of $^{177}$Lu-PSMA-617 in patients with metastatic castration-resistant prostate cancer. Cureus 2020; 12: e8921.
[112] von Eyben FE, Bauman G, von Eyben R, Rahbar K, Soydal C, Haug AR, Virgolini I, Kulkarni H, Baum R and Paganelli G. Optimizing PSMa radioligand therapy for patients with metastatic castration-resistant prostate cancer. a systematic review and meta-analysis. Int J Mol Sci 2020; 21: 9054.
[113] Weber M, Hadaschik B, Ferdinandus J, Rahbar K, Bögemann M, Herrmann K, Fendler WP and Kesch C. Prostate-specific membrane antigen-based imaging of castration-resistant prostate cancer. Eur Urol Focus 2021; 7: 279-287.
[114] Wester HJ and Schottelius M. PSMA-targeted radiopharmaceuticals for imaging and therapy. Semin Nucl Med 2019; 49: 302-312.
[115] Zang J, Liu Q, Sui H, Wang R, Jacobson O, Fan X, Zhu Z and Chen X. $^{177}$Lu-EB-PSMA radioligand therapy with escalating doses in patients with metastatic castration-resistant prostate cancer. J Nucl Med 2020; 61: 1772-1778.
[116] von Eyben FE, Roviello G, Kiljunen T, Uprimny C, Virgolini I, Kairemo K and Joensuu T. Third-line treatment and $^{177}$Lu-PSMA radioligand therapy of metastatic castration-resistant prostate cancer: a systematic review. Eur J Nucl Med Mol Imaging 2018; 45: 496-508.
[117] Chakraborty S, Chakravarty R, Shetty P, Vimalnath KV, Sen IB and Dash A. Prospects of medium specific activity $^{177}$Lu in targeted therapy of prostate cancer using $^{177}$Lu-labeled PSMA inhibitor. J Labelled Comp Radiopharm 2016; 59: 364-371.
[118] Chakraborty S, Vimalnath KV, Chakravarty R, Sarma HD and Dash A. Multidose formulation of ready-to-use $^{177}$Lu-PSMA-617 in a centralized radiopharmacy set-up. Appl Radiat Isot 2018; 139: 91-97.
[119] Yadav MP, Ballal S, Tripathi M, Damle NA, Sahoo RK, Seth A and Bal C. Post-therapeutic dosimetry of $^{177}$Lu-DKFZ-PSMA-617 in the treatment of patients with metastatic castration-resistant prostate cancer. Nucl Med Commun 2017; 38: 91-98.
[120] Yadav MP, Ballal S, Tripathi M, Damle NA, Sahoo RK, Seth A and Bal C. $^{177}$Lu-DKFZ-PS-

MA-617 therapy in metastatic castration resistant prostate cancer: safety, efficacy, and quality of life assessment. Eur J Nucl Med Mol Imaging 2017; 44: 81-91.
[121] Suman S, Parghane RV, Joshi A, Prabhash K, Bakshi G, Talole S, Banerjee S and Basu S. Therapeutic efficacy, prognostic variables and clinical outcome of $^{177}$Lu-PSMA-617 PRLT in progressive mCRPC following multiple lines of treatment: prognostic implications of high FDG uptake on dual tracer PET-CT vis-à-vis Gleason score in such cohort. Br J Radiol 2019; 92: 20190380.
[122] Adnan A and Basu S. Comparison of dual-tracer PET and CT features to conventional risk categories in assessing response to $^{177}$Lu-PSMA-617 therapy for metastatic prostate adenocarcinoma with urinary bladder involvement. J Nucl Med Technol 2020; 48: 148-153.
[123] Kattepur AK, Gulia A, Jones RL and Rastogi S. Extraskeletal osteosarcomas: current update. Future Oncol 2021; 17: 825-835.
[124] Liu F, Ke J and Song Y. Application of biomarkers for the prediction and diagnosis of bone metastasis in breast cancer. J Breast Cancer 2020; 23: 588-598.
[125] Marques C, Roberts C, Matos VMJ and Buikstra JE. Cancers as rare diseases: terminological, theoretical, and methodological biases. Int J Paleopathol 2021; 32: 111-122.
[126] Mollica V, Rizzo A, Rosellini M, Marchetti A, Ricci AD, Cimadamore A, Scarpelli M, Bonucci C, Andrini E, Errani C, Santoni M, Montironi R and Massari F. Bone targeting agents in patients with metastatic prostate cancer: state of the art. Cancers (Basel) 2021; 13: 546.
[127] Peters C, Vandewiele J, Lievens Y, van Eijkeren M, Fonteyne V, Boterberg T, Deseyne P, Veldeman L, De Neve W, Monten C, Braems S, Duprez F, Vandecasteele K and Ost P. Adoption of single fraction radiotherapy for uncomplicated bone metastases in a tertiary centre. Clin Transl Radiat Oncol 2021; 27: 64-69.
[128] Soni S, Torvund M and Mandal CC. Molecular insights into the interplay between adiposity, breast cancer and bone metastasis. Clin Exp Metastasis 2021; 38: 119-138.
[129] Dash A, Das T and Knapp FFR. Targeted radionuclide therapy of painful bone metastases: past developments, current status, recent advances and future directions. Curr Med Chem 2020; 27: 3187-3249.
[130] Bouman-Wammes EW, de Klerk JMH, Bloemendal HJ, Van Dodewaard-de Jong JM, Lange R, Ter Heine R, Verheul HMW and Van den Eertwegh AJM. Bone-targeting radiopharmaceuticals as monotherapy or combined with chemotherapy in patients with castration-resistant prostate cancer metastatic to bone. Clin Genitourin Cancer 2019; 17: e281-e292.
[131] Manafi-Farid R, Masoumi F, Divband G, Saidi B, Ataeinia B, Hertel F, Schweighofer-Zwink G, Morgenroth A and Beheshti M. Targeted palliative radionuclide therapy for metastatic bone pain. J Clin Med 2020; 9: 2622.
[132] Miranda J, Viñal D and Pinto Á. Radium 223 for the treatment of metastatic castration-resistant prostate cancer. Arch Esp Urol 2019; 72: 500-507.
[133] Murray I and Du Y. Systemic radiotherapy of bone metastases with radionuclides. Clin Oncol (R Coll Radiol) 2021; 33: 98-105.
[134] Sadremomtaz A and Masoumi M. An assessment of bone-seeking radionuclides for palliation of metastatic bone pain in a vertebral model. Ann Nucl Med 2019; 33: 252-264.
[135] Wada Y, Anbai A, Kumagai S, Okuyama E, Hatakeyama K, Takagi N and Hashimoto M. Effect of the types of pretreatment imaging modalities on the treatment response to palliative radiation for painful bone metastases from solid cancer: a single-center retrospective analysis. Radiat Oncol 2019; 14: 98.
[136] Bal C, Arora G, Kumar P, Damle N, Das T, Chakraborty S, Banerjee S, Venkatesh M, Zaknun JJ and Pillai MR. Pharmacokinetic, dosimetry and toxicity study of $^{177}$Lu-EDTMP in patients: phase 0/I study. Curr Radiopharm 2016; 9: 71-84.
[137] Agarwal KK, Singla S, Arora G and Bal C. $^{177}$Lu-EDTMP for palliation of pain from bone metastases in patients with prostate and breast cancer: a phase II study. Eur J Nucl Med Mol Imaging 2015; 42: 79-88.
[138] Thapa P, Nikam D, Das T, Sonawane G, Agarwal JP and Basu S. Clinical efficacy and safety comparison of $^{177}$Lu-EDTMP with $^{153}$Sm-EDTMP on an equidose basis in patients with painful skeletal metastases. J Nucl Med 2015; 56: 1513-1519.
[139] Sharma S, Singh B, Koul A and Mittal BR. Comparative therapeutic efficacy of $^{153}$Sm-EDTMP and $^{177}$Lu-EDTMP for bone pain palliation in patients with skeletal metastases: patients' pain score analysis and personalized dosimetry. Front Med (Lausanne) 2017; 4: 46.
[140] Chakraborty S, Das T, Sarma HD, Venkatesh M and Banerjee S. Comparative studies of $^{177}$Lu-EDTMP and $^{177}$Lu-DOTMP as potential agents for palliative radiotherapy of bone metastasis. Appl Radiat Isot 2008; 66: 1196-1205.
[141] Bollampally N, Shukla J, Mittal BR, Sood A, Mohanty M, Kapoor R, Vatsa R, Satapathy S, Chakravarty R, Chakraborty S and Dash AK. Efficacy and safety of $^{177}$Lu-DOTMP in palliative treatment of symptomatic skeletal metastases: a prospective study. Nucl Med Commun 2021; 42: 964-971.
[142] Keeling GP, Sherin B, Kim J, San Juan B, Grus T, Eykyn TR, Rösch F, Smith GE, Blower PJ, Terry

SYA and T M de Rosales R. [$^{68}$Ga]Ga-THP-Pam: a bisphosphonate PET tracer with facile radiolabeling and broad calcium mineral affinity. Bioconjug Chem 2020; 32: 1276-1289.
[143] Meckel M, Fellner M, Thieme N, Bergmann R, Kubicek V and Rösch F. In vivo comparison of DOTA based $^{68}$Ga-labelled bisphosphonates for bone imaging in non-tumour models. Nucl Med Biol 2013; 40: 823-830.
[144] Meckel M, Kubíček V, Hermann P, Miederer M and Rösch F. A DOTA based bisphosphonate with an albumin binding moiety for delayed body clearance for bone targeting. Nucl Med Biol 2016; 43: 670-678.
[145] Meckel M, Nauth A, Timpe J, Zhernosekov K, Puranik AD, Baum RP and Rösch F. Development of a [$^{177}$Lu]BPAMD labeling kit and an automated synthesis module for routine bone targeted endoradiotherapy. Cancer Biother Radiopharm 2015; 30: 94-99.
[146] Pfannkuchen N, Meckel M, Bergmann R, Bachmann M, Bal C, Sathekge M, Mohnike W, Baum RP and Rösch F. Novel radiolabeled bisphosphonates for PET diagnosis and endoradiotherapy of bone metastases. Pharmaceuticals (Basel) 2017; 10: 45.
[147] Rabie A, Enayati R, Yousefnia H, Jalilian AR, Shamsaei M, Zolghadri S, Bahrami-Samani A and Hosntalab M. Preparation, quality control and biodistribution assessment of $^{153}$Sm-BPAMD as a novel agent for bone pain palliation therapy. Ann Nucl Med 2015; 29: 870-876.
[148] Wu Z, Zha Z, Choi SR, Plössl K, Zhu L and Kung HF. New $^{68}$Ga-PhenA bisphosphonates as potential bone imaging agents. Nucl Med Biol 2016; 43: 360-371.
[149] Chakraborty S, Shetty P, Chakravarty R, Vimalnath KV, Kumar C, Sarma HD, Vatsa R, Shukla J, Mittal BR and Dash A. Formulation of 'ready-to-use' human clinical doses of $^{177}$Lu-labeled bisphosphonate amide of DOTA using moderate specific activity $^{177}$Lu and its preliminary evaluation in human patient. Radiochim Acta 2020; 108: 661-672.
[150] Palma E, Correia JD, Campello MP and Santos I. Bisphosphonates as radionuclide carriers for imaging or systemic therapy. Mol Biosyst 2011; 7: 2950-2966.
[151] Russell RG, Watts NB, Ebetino FH and Rogers MJ. Mechanisms of action of bisphosphonates: similarities and differences and their potential influence on clinical efficacy. Osteoporos Int 2008; 19: 733-759.
[152] Fernandez R, Eppard E, Lehnert W, Jimenez-Franco LD, Soza-Ried C, Ceballos M, Ribbeck J, Kluge A, Roesch F, Meckel M, Zhernosekov K, Kramer V and Amaral H. Evaluation of safety and dosimetry of $^{177}$Lu DOTA-ZOL for therapy of bone metastases. J Nucl Med 2021; 62: 1126-1132.
[153] Khawar A, Eppard E, Roesch F, Ahmadzadehfar H, Kürpig S, Meisenheimer M, Gaertner FC, Essler M and Bundschuh RA. Biodistribution and post-therapy dosimetric analysis of [$^{177}$Lu]Lu-DOTA(ZOL) in patients with osteoblastic metastases: first results. EJNMMI Res 2019; 9: 102.
[154] Khawar A, Eppard E, Roesch F, Ahmadzadehfar H, Kürpig S, Meisenheimer M, Gaertner FC, Essler M and Bundschuh RA. Preliminary results of biodistribution and dosimetric analysis of [$^{68}$Ga]Ga-DOTA(ZOL): a new zoledronate-based bisphosphonate for PET/CT diagnosis of bone diseases. Ann Nucl Med 2019; 33: 404-413.
[155] Meckel M, Bergmann R, Miederer M and Roesch F. Bone targeting compounds for radiotherapy and imaging: *Me(III)-DOTA conjugates of bisphosphonic acid, pamidronic acid and zoledronic acid. EJNMMI Radiopharm Chem 2017; 1: 14.
[156] Meisenheimer M, Kürpig S, Essler M and Eppard E. DOTA-ZOL: a promising tool in diagnosis and palliative therapy of bone metastasis-challenges and critical points in implementation into clinical routine. Molecules 2020; 25: 2988.
[157] Yadav MP, Ballal S, Meckel M, Roesch F and Bal C. [$^{177}$Lu]Lu-DOTA-ZOL bone pain palliation in patients with skeletal metastases from various cancers: efficacy and safety results. EJNMMI Res 2020; 10: 130.
[158] Shi J, Fan D, Dong C, Liu H, Jia B, Zhao H, Jin X, Liu Z, Li F and Wang F. Anti-tumor effect of integrin targeted $^{177}$Lu-3PRGD2 and combined therapy with endostar. Theranostics 2014; 4: 256-266.
[159] Luna-Gutiérrez M, Ferro-Flores G, Ocampo-García B, Jiménez-Mancilla N, Morales-Avila E, De León-Rodríguez L and Isaac-Olivé K. $^{177}$Lu-labeled monomeric, dimeric and multimeric RGD peptides for the therapy of tumors expressing $\alpha_v\beta_3$ integrins. J Labelled Comp Radiopharm 2012; 55: 140-148.
[160] Chakraborty S, Sarma HD, Vimalnath KV and Pillai MR. Tracer level radiochemistry to clinical dose preparation of $^{177}$Lu-labeled cyclic RGD peptide dimer. Nucl Med Biol 2013; 40: 946-954.
[161] Parihar AS, Sood A, Kumar R, Bhusari P, Shukla J and Mittal BR. Novel use of $^{177}$Lu-DOTA-RGD$_2$ in treatment of $^{68}$Ga-DOTA-RGD$_2$-avid lesions in papillary thyroid cancer with TENIS. Eur J Nucl Med Mol Imaging 2018; 45: 1836-1837.
[162] Camacho X, Calzada V, Fernandez M, Alonso O, Chammas R, Riva E, Gambini JP and Cabral

P. $^{177}$Lu-DOTA-bevacizumab: radioimmunotherapy agent for melanoma. Curr Radiopharm 2017; 10: 21-28.
[163] Deshayes E, Ladjohounlou R, Le Fur P, Pichard A, Lozza C, Boudousq V, Sevestre S, Jarlier M, Kashani R, Koch J, Sosabowski J, Foster J, Chouin N, Bruchertseifer F, Morgenstern A, Kotzki PO, Navarro-Teulon I and Pouget JP. Radiolabeled antibodies against müllerian-inhibiting substance receptor, type II: new tools for a theranostic approach in ovarian cancer. J Nucl Med 2018; 59: 1234-1242.
[164] Minnix M, Adhikarla V, Caserta E, Poku E, Rockne R, Shively JE and Pichiorri F. Comparison of CD38 targeted alpha- vs beta-radionuclide therapy of disseminated multiple myeloma in an animal model. J Nucl Med 2020; 62:795-801.
[165] Mortensen AC, Spiegelberg D, Haylock AK, Lundqvist H and Nestor M. Preclinical evaluation of a novel engineered recombinant human anti-CD44v6 antibody for potential use in radio-immunotherapy. Int J Oncol 2018; 52: 1875-1885.
[166] Timmermand OV, Elgqvist J, Beattie KA, Örbom A, Larsson E, Eriksson SE, Thorek DLJ, Beattie BJ, Tran TA, Ulmert D and Strand SE. Preclinical efficacy of hK2 targeted [(177)Lu]hu11B6 for prostate cancer theranostics. Theranostics 2019; 9: 2129-2142.
[167] Chakravarty R, Chakraborty S, Sarma HD, Nair KV, Rajeswari A and Dash A. $^{90}$Y/$^{177}$Lu-labelled Cetuximab immunoconjugates: radiochemistry optimization to clinical dose formulation. J Labelled Comp Radiopharm 2016; 59: 354-363.
[168] Chakravarty R, Rohra N, Chakraborty S, Jain R, Sarma HD and Dash A. Clinically relevant radioactive dose formulation of $^{177}$Lu-labeled cetuximab-fab fragment for potential use in cancer theranostics. Chem Select 2018; 3: 242-248.
[169] Kang L, Li C, Rosenkrans ZT, Huo N, Chen Z, Ehlerding EB, Huo Y, Ferreira CA, Barnhart TE, Engle JW, Wang R, Jiang D, Xu X and Cai W. CD38-targeted theranostics of lymphoma with $^{89}$Zr/$^{177}$Lu-labeled daratumumab. Adv Sci (Weinh) 2021; 8: 2001879.
[170] Yadav MP, Singla S, Thakral P, Ballal S and Bal C. Dosimetric analysis of 177Lu-DOTA-rituximab in patients with relapsed/refractory non-Hodgkin's lymphoma. Nucl Med Commun 2016; 37: 735-742.
[171] Bhusari P, Vatsa R, Singh G, Parmar M, Bal A, Dhawan DK, Mittal BR and Shukla J. Development of Lu-177-trastuzumab for radioimmunotherapy of HER2 expressing breast cancer and its feasibility assessment in breast cancer patients. Int J Cancer 2017; 140: 938-947.
[172] Ahmad I and Nisar H. Dosimetry perspectives in radiation synovectomy. Phys Med 2018; 47: 64-72.
[173] García-Colmenero L, Martin-Ezquerra G, Monfort J and Pujol RM. Persistent cutaneous ulcers after Yttrium-90 synovectomy, an unusual complication: two case reports and a review of the literature. Int Wound J 2017; 14: 508-511.
[174] Kitonyi GW and Kitonyi JM. Radiation synovectomy: treatment option for haemophilia patients with chronic haemarthrosis: a review. East Afr Med J 2009; 86 Suppl: S71-75.
[175] Knut L. Radiosynovectomy in the therapeutic management of arthritis. World J Nucl Med 2015; 14: 10-15.
[176] Lopez-Olivo MA, Kakpovbia-Eshareturi V, des Bordes JK, Barbo A, Christensen R and Suarez-Almazor ME. Treating early undifferentiated arthritis: a systematic review and meta-analysis of direct and indirect trial evidence. Arthritis Care Res (Hoboken) 2018; 70: 1355-1365.
[177] Mollon B, Lee A, Busse JW, Griffin AM, Ferguson PC, Wunder JS and Theodoropoulos J. The effect of surgical synovectomy and radiotherapy on the rate of recurrence of pigmented villonodular synovitis of the knee: an individual patient meta-analysis. Bone Joint J 2015; 97-B: 550-557.
[178] Rodriguez-Merchan EC. Radiosynovectomy in haemophilia. Blood Rev 2019; 35: 1-6.
[179] Teyssler P, Kolostova K and Bobek V. Radionuclide synovectomy in haemophilic joints. Nucl Med Commun 2013; 34: 291-297.
[180] van der Zant FM, Boer RO, Moolenburgh JD, Jahangier ZN, Bijlsma JW and Jacobs JW. Radiation synovectomy with (90)Yttrium, (186) Rhenium and (169)Erbium: a systematic literature review with meta-analyses. Clin Exp Rheumatol 2009; 27: 130-139.
[181] Chakraborty S, Vimalnath KV, Rajeswari A, Shinto A, Sarma HD, Kamaleshwaran K, Thirumalaisamy P and Dash A. Preparation, evaluation, and first clinical use of 177Lu-labeled hydroxyapatite (HA) particles in the treatment of rheumatoid arthritis: utility of cold kits for convenient dose formulation at hospital radiopharmacy. J Labelled Comp Radiopharm 2014; 57: 453-462.
[182] Shinto AS, Kamaleshwaran KK, Chakraborty S, Vyshakh K, Thirumalaisamy SG, Karthik S, Nagaprabhu VN, Vimalnath KV, Das T and Banerjee S. Radiosynovectomy of painful synovitis of knee joints due to rheumatoid arthritis by intra-articular administration of $^{177}$Lu-labeled hydroxyapatite particulates: first human study and initial indian experience. World J Nucl Med 2015; 14: 81-88.
[183] Arora G, Singh M, Jha P, Tripathy S, Bal C, Mukherjee A and Shamim SA. Formulation and characterization of lutetium-177-labeled stannous (tin) colloid for radiosynovectomy. Nucl Med Commun 2017; 38: 587-592.
[184] Jha P, Arora G, Shamim SA, Mukherjee A, Gautam D, Ballal S, Kumar U, Ansari TM and Bal C.

Lutetium-177 tin colloid radiosynovectomy in patients with inflammatory knee joint conditions intractable to prevailing therapy. Nucl Med Commun 2018; 39: 803-808.
[185] Shamim SA, Arora G, Jha P, Gupta P, Behera A, Mukherjee A, Prabhu M, Ansari MT, Vyas S and Bal C. Comparison of Lutetium-177 tin colloid and Rhenium-188 tin colloid radiosynovectomy in chronic knee arthritis. Nucl Med Commun 2020; 41: 721-726.
[186] Andreou C, Pal S, Rotter L, Yang J and Kircher MF. Molecular imaging in nanotechnology and theranostics. Mol Imaging Biol 2017; 19: 363-372.
[187] Aranda-Lara L, Morales-Avila E, Luna-Gutiérrez MA, Olivé-Alvarez E and Isaac-Olivé K. Radiolabeled liposomes and lipoproteins as lipidic nanoparticles for imaging and therapy. Chem Phys Lipids 2020; 230: 104934.
[188] Datta P and Ray S. Nanoparticulate formulations of radiopharmaceuticals: strategy to improve targeting and biodistribution properties. J Labelled Comp Radiopharm 2020; [Epub ahead of print].
[189] Forte E, Fiorenza D, Torino E, Costagliola di Polidoro A, Cavaliere C, Netti PA, Salvatore M and Aiello M. Radiolabeled PET/MRI nanoparticles for tumor imaging. J Clin Med 2019; 9: 89.
[190] Frantellizzi V, Conte M, Pontico M, Pani A, Pani R and De Vincentis G. New frontiers in molecular imaging with superparamagnetic iron oxide nanoparticles (SPIONs): efficacy, toxicity, and future applications. Nucl Med Mol Imaging 2020; 54: 65-80.
[191] Holzwarth U, Ojea Jimenez I and Calzolai L. A random walk approach to estimate the confinement of α-particle emitters in nanoparticles for targeted radionuclide therapy. EJNMMI Radiopharm Chem 2018; 3: 9.
[192] Jeon J. Review of therapeutic applications of radiolabeled functional nanomaterials. Int J Mol Sci 2019; 20: 2323.
[193] Ni D, Jiang D, Ehlerding EB, Huang P and Cai W. Radiolabeling silica-based nanoparticles via coordination chemistry: basic principles, strategies, and applications. Acc Chem Res 2018; 51: 778-788.
[194] Pellico J, Gawne PJ and T M de Rosales R. Radiolabelling of nanomaterials for medical imaging and therapy. Chem Soc Rev 2021; 50: 3355-3423.
[195] Peltek OO, Muslimov AR, Zyuzin MV and Timin AS. Current outlook on radionuclide delivery systems: from design consideration to translation into clinics. J Nanobiotechnology 2019; 17: 90.
[196] Polyak A and Ross TL. Nanoparticles for SPECT and PET imaging: towards personalized medicine and theranostics. Curr Med Chem 2018; 25: 4328-4353.
[197] Ranjbar Bahadori S, Mulgaonkar A, Hart R, Wu CY, Zhang D, Pillai A, Hao Y and Sun X. Radiolabeling strategies and pharmacokinetic studies for metal based nanotheranostics. Wiley Interdiscip Rev Nanomed Nanobiotechnol 2021; 13: e1671.
[198] Silva F, Cabral Campello MP and Paulo A. Radiolabeled gold nanoparticles for imaging and therapy of cancer. Materials (Basel) 2020; 14: 4.
[199] Arora G, Shukla J, Ghosh S, Maulik SK, Malhotra A and Bandopadhyaya G. PLGA nanoparticles for peptide receptor radionuclide therapy of neuroendocrine tumors: a novel approach towards reduction of renal radiation dose. PLoS One 2012; 7: e34019.
[200] Arora G, Dubey P, Shukla J, Ghosh S and Bandopadhyaya G. Evaluation of cytotoxic and tumor targeting capability of $^{177}$Lu-DOTATATE-nanoparticles: a trailblazing strategy in peptide receptor radionuclide therapy. Ann Nucl Med 2016; 30: 334-345.
[201] Chakravarty R, Chakraborty S, Guleria A, Kumar C, Kunwar A, Nair KVV, Sarma HD and Dash A. Clinical scale synthesis of intrinsically radiolabeled and cyclic RGD peptide functionalized $^{198}$Au nanoparticles for targeted cancer therapy. Nucl Med Biol 2019; 72-73: 1-10.
[202] Chen D, Yang D, Dougherty CA, Lu W, Wu H, He X, Cai T, Van Dort ME, Ross BD and Hong H. In vivo targeting and positron emission tomography imaging of tumor with intrinsically radioactive metal-organic frameworks nanomaterials. ACS Nano 2017; 11: 4315-4327.
[203] Chen F, Valdovinos HF, Hernandez R, Goel S, Barnhart TE and Cai W. Intrinsic radiolabeling of Titanium-45 using mesoporous silica nanoparticles. Acta Pharmacol Sin 2017; 38: 907-913.
[204] Heo GS, Zhao Y, Sultan D, Zhang X, Detering L, Luehmann HP, Zhang X, Li R, Choksi A, Sharp S, Levingston S, Primeau T, Reichert DE, Sun G, Razani B, Li S, Weilbaecher KN, Dehdashti F, Wooley KL and Liu Y. Assessment of copper nanoclusters for accurate in vivo tumor imaging and potential for translation. ACS Appl Mater Interfaces 2019; 11: 19669-19678.
[205] Lamb J and Holland JP. Advanced methods for radiolabeling multimodality nanomedicines for SPECT/MRI and PET/MRI. J Nucl Med 2018; 59: 382-389.
[206] Wall MA, Shaffer TM, Harmsen S, Tschaharganeh DF, Huang CH, Lowe SW, Drain CM and Kircher MF. Chelator-free radiolabeling of SERRS nanoparticles for whole-body PET and intraoperative raman imaging. Theranostics 2017; 7: 3068-3077.

[207] Zhan Y, Ehlerding EB, Shi S, Graves SA, Goel S, Engle JW, Liang J and Cai W. Intrinsically zirconium-89-labeled manganese oxide nanoparticles for in vivo dual-modality positron emission tomography and magnetic resonance imaging. J Biomed Nanotechnol 2018; 14: 900-909.

[208] Chakravarty R, Chakraborty S, Ningthoujam RS, Vimalnath Nair KV, Sharma KS, Ballal A, Guleria A, Kunwar A, Sarma HD, Vatsa RK and Dash A. Industrial-scale synthesis of intrinsically radiolabeled $^{64}$CuS nanoparticles for use in positron emission tomography (PET) imaging of cancer. Ind Eng Chem Res 2016; 55: 12407-12419.

[209] Chakravarty R, Chakraborty S, Guleria A, Kunwar A, Sarma HD and Dash A. Facile one-pot synthesis of intrinsically radiolabeled $^{64}$Cu-human serum albumin nanocomposite for cancer targeting. Chem Select 2017; 2: 8043-8051.

[210] Chakravarty R, Chakraborty S, Guleria A, Shukla R, Kumar C, Vimalnath Nair KV, Sarma HD, Tyagi AK and Dash A. Facile one-pot synthesis of intrinsically radiolabeled and cyclic RGD conjugated $^{199}$Au nanoparticles for potential use in nanoscale brachytherapy. Ind Eng Chem Res 2018; 57: 14337-14346.

[211] Chakravarty R, Guleria A, Jadhav S, Kumar C, Debnath AK, Sarma HD and Chakraborty S. Bioinspired synthesis of intrinsically $^{177}$Lu-labeled hybrid nanoparticles for potential cancer therapy. Ind Eng Chem Res 2020; 59: 22492-22500.

[212] Zhang X, Chen F, Turker MZ, Ma K, Zanzonico P, Gallazzi F, Shah MA, Prater AR, Wiesner U, Bradbury MS, McDevitt MR and Quinn TP. Targeted melanoma radiotherapy using ultrasmall $^{177}$Lu-labeled α-melanocyte stimulating hormone-functionalized core-shell silica nanoparticles. Biomaterials 2020; 241: 119858.

[213] Chen F, Goel S, Hernandez R, Graves SA, Shi S, Nickles RJ and Cai W. Dynamic positron emission tomography imaging of renal clearable gold nanoparticles. Small 2016; 12: 2775-2782.

[214] Cheng L, Jiang D, Kamkaew A, Valdovinos HF, Im HJ, Feng L, England CG, Goel S, Barnhart TE, Liu Z and Cai W. Renal-clearable PEGylated porphyrin nanoparticles for image-guided photodynamic cancer therapy. Adv Funct Mater 2017; 27: 1702928.

[215] Ehlerding EB, Chen F and Cai W. Biodegradable and renal clearable inorganic nanoparticles. Adv Sci (Weinh) 2016; 3: 1500223.

[216] Shen S, Jiang D, Cheng L, Chao Y, Nie K, Dong Z, Kutyreff CJ, Engle JW, Huang P, Cai W and Liu Z. Renal-clearable ultrasmall coordination polymer nanodots for chelator-free $^{64}$Cu-labeling and imaging-guided enhanced radiotherapy of cancer. ACS Nano 2017; 11: 9103-9111.